Response to Editor's comments to manuscript essd-2020-57

"Annual 30-meter Dataset for Glacial Lakes in High Mountain Asia from 2008 to 2017"

Dear Editor:

Thank you a lot for your kind and careful reviewing. Your suggestions give us important and constructive perspective on this manuscript, and help to improve the manuscript greatly. We have fully considered all the comments of you, and have substantially revised our manuscript according to your comments. A point-by-point response to the outstanding comments raised is attached to this manuscript. The major changes are summarized as follows:

1. We have been looking for a native speaker and a special Polish Company: Charlesworth to modify the paper, and to reduce the language and grammar errors as possible.

2. The full term of every acronym has been introduced the first time it was used in the manuscript.

3. We have modified the data description document by adding the content about data sources and methods, spelling out all the abbreviations of the table caption, and adding the ORCID details of all the authors.

4. The CRS of all the prj files of our dataset have been transformed into a standard projection Asia_North_Albers_Equal_Area_Conic (ESRI: 102025) according to the spatialreference.org.

The changes can be tracked in the revised manuscript. In the following, we provide point by point responses to the outstanding comments and suggestions provided by the Topical editor. We are indebted to you for your outstanding and constructive comments, which greatly helped us to improve the technical quality and presentation of our manuscript. Once again, thank you very much for your comments and suggestions.

Response to Comments by Topical editor:

1. *The published time series on Glacial Lakes in High Mountain Asia is of importance. The manuscript, the data description and data publication do not yet fulfill the requirements of ESSD and improvements are needed. A major revision of the manuscript and a minor revision of the dataset is needed.*

   First, the manuscript requires editing by a professional English language editing service. SRTM, SLC, GAMDAM and many more acronyms are not introduced. Introduce every acronym before using it in the text. The first time you use the term, put the acronym in parentheses after the full term. Please upload the revised version of your manuscript with track changes included.

Response:

We greatly appreciate the suggestions of the Topical editor for his/her accurate summary of the main contributions of our work and for the outstanding recommendations provided. Following the Topical editor's very pertinent recommendations, in the revised manuscript and the following text we have made modifications according to these questions. We thank again the Topical editor for his/her careful handling of our manuscript and for the constructive suggestions provided, which greatly helped us improve the technical quality and presentation of our manuscript.

We have been looking for a native speaker and a special Polish Company: Charlesworth to modify the paper, and to reduce the language and grammar errors as possible. Then we have corrected all the acronyms by introducing the full term first and put the acronym in parentheses. Besides, the revised version of manuscript is uploaded with track changes included.

2. *Please also optimize the data set abstract in Zenodo, please include data sources and methods in the abstract.*

   Please also include data sources and methods in the data description document. Please add the overview on the dBASE table in the overview text, please spell out abbreviations, e.g. GL_type in the table caption. Please add your ORCID in the data description document.

Response:

Thanks for these good suggestions. Firstly, we have optimized the data set abstract in Zenodo by adding the content about data sources and methods. The detailed modifications are as follows:

We developed a High Mountain Asia (HMA) Glacial Lake Inventory (Hi-MAG) database to characterize the annual coverage of glacial lakes from 2008 to 2017 at 30 m resolution. For the development of the Hi-MAG database, a total of 40,481 satellite images including Landsat 5 TM, Landsat 7 ETM+ and Landsat 8 OLI were used, and a systematic glacial lake detection method that comprised the automated processing using GEE and subsequent manual refinement of these lake mapping results were applied. This is the first glacial lake inventory across the HMA with annual temporal resolution, it can provide details for different types of glacial lakes and evolution patterns. It can be used for studies of the complex interactions between glaciers, climate, and glacial lakes, and GLOFs, potential downstream risks, and water resources.

Then the information about the data sources and methods have also been added in **the Section of Brief introduction** of the data description document.

Finally, we have modified the data description document by adding the overview about the dBASE table, spelling out all the abbreviations of the table caption, and adding the ORCID details of all the authors. The detailed modifications are as follows:

2) Hi-MAG database.zip: it contains 50 files in total for the ten years. Each phase consists of five files, including *.shp (the main file that stores the feature geometry), *.shx (the index file that stores the index of the feature geometry), *.dbf (the dBASE table that stores the attribute information of features, including **GL_ID**: the coding of glacial lake, **GL_type**: the type of glacial lake, **GL_Area**: the area of glacial lake (m^2), **GL_Year**: the year of mapped glacial lake, **GL_Elev**: the elevation of glacial lake (m), **GL_SubR**: the sub-region of glacial lake in the HMA, **GL_Peri**: the perimeter of glacial lake (m),

Distance: the euclidian distance from glacial lake to the nearest glacier terminus (m)), *cpg (character encoding file, describes a set of characters for displaying text in shapefiles; helps localize maps for specific languages), and *.prj (the file that stores the coordinate system information). In each shape file, the polygons are boundaries of each glacial lake.

Authors:

Fang Chen (chenfang@radi.ac.cn) https://orcid.org/0000-0002-3245-2584

Meimei Zhang (zhangmm@radi.ac.cn) https://orcid.org/0000-0001-9621-4879

Huadong Guo (hdguo@radi.ac.cn) https://orcid.org/0000-0003-0337-1862

Simon Allen (simon.allen@geo.uzh.ch) https://orcid.org/0000-0002-4809-649X

Jeffrey S. Kargel (jeffreyskargel@hotmail.com) https://orcid.org/0000-0002-5506-1797

Umesh K. Haritashya (uharitashya1@udayton.edu) https://orcid.org/0000-0001-9527-954X

C. Scott Watson (cswatson@email.arizona.edu) https://orcid.org/0000-0003-2656-961X

3. *ESSD policy requires the re-usability of the published data sets using open source: Please list open-source GIS software in the list of software. Using open source GIS software, e.g. QGIS, the CRS of Glacial Lakes in High Mountain Asia is not readily recognized, eventually because it is no standard projection. Could you check back with spatialreference.org, eventually change your prj file.*

   e.g.https://essd.copernicus.org/articles/10/2275/2018/essd-10-2275-2018.pdf Carlson and Oda put the example of QGIS-compatible shapefiles.

Response:

We gratefully thank the Topical editor for his/her comments and suggestions. We have listed the open-source GIS software in the **Section 6. Recommended software** of the data description document. The detailed modifications are as follows:

6. Recommended software

All the vector (shape) files of this dataset can be easily opened and processed with QGIS, gvSIG or other open-source remote sensing and geographic information system software.

Besides, the CRS of our last version of dataset is not recognized by QGIS software indeed, which is due to the fact that it is a custom coordinate system, rather than a standard projection. Therefore, following the Topical editor's very pertinent recommendations, we have carefully changed all the prj files by transforming their CRS to standard Asia_North_Albers_Equal_Area_Conic (ESRI: 102025) according to the spatialreference.org.

Annual 30-meter Dataset for Glacial Lakes in High Mountain Asia from 2008 to 2017

Fang Chen[1,2,3], Meimei Zhang[1], Huadong Guo[1,2,3], Simon Allen[4,5], Jeffrey S. Kargel[6], Umesh K. Haritashya[7], C. Scott Watson[8]

[1]Key Laboratory of Digital Earth Science, Aerospace Information Research Institute, Chinese Academy of Sciences, No. 9 Dengzhuang South Road, Beijing 100094, China.

[2]State Key Laboratory of Remote Sensing Science, Aerospace Information Research Institute, Chinese Academy of Sciences, No. 9 Dengzhuang South Road, Beijing 100094, China.

[3]Hainan Key Laboratory of Earth Observation, Aerospace Information Research Institute, Chinese Academy of Sciences, Sanya 572029, China.

[4]Department of Geography, University of Zurich, Zurich, 8057, Switzerland.

[5]Institute for Environmental Sciences, University of Geneva, Geneva 1205, Switzerland.

[6]The Planetary Science Institute, Tucson, Arizona, 85719, USA.

[7]Department of Geology, University of Dayton, Dayton, Ohio, 45469, USA.

[8]Department of Hydrology & Atmospheric Sciences, University of Arizona, Tucson, Arizona, 85721, USA.

Correspondence to: Meimei Zhang (zhangmm@radi.ac.cn)

Abstract. Atmospheric warming is intensifying glacier melting and glacial lake development in High Mountain Asia (HMA), ~~which~~and this could increase glacial lake outburst flood (GLOF) hazards and impact water ~~resource~~resources and hydroelectric power management. There is therefore a pressing need ~~for obtaining the~~to obtain comprehensive knowledge of the distribution~~,~~ and area of glacial lakes, and also ~~quantification of~~ to quantify the variability in their ~~size~~sizes and ~~type~~types at high resolution in HMA. ~~Here~~In this work, we developed ~~a~~an HMA ~~Glacial Lake Inventory~~glacial lake inventory (Hi-MAG) database to characterize the annual coverage of glacial lakes from 2008 to 2017 at 30 ~~-~~m resolution using Landsat satellite imagery. ~~It can be observed~~Our data show that glacial lakes exhibited a total area ~~increases~~increase of 90.14 ~~-~~ km^2 ~~between~~in the period 2008 ~~-~~2017, a +6.90% change relative to 2008 (1305.59~~±~~ ± 213.99 ~~-~~ km^2). ~~Annual increase~~The annual increases in ~~lake~~the number and area ~~are 306 glacial~~ of lakes were 306 and 12 ~~-~~ km^2, respectively, and ~~maximum increased lake~~ the greatest increase in the number of lakes occurred in 5400 m elevation, which increased by 249. Proglacial ~~-~~ lake ~~-~~ dominated areas, such as the ~~Nyainqentanglha~~Nyainqêntanglha and Central Himalaya, where ~~around~~ more than half of the glacial lake area (summed over a 1° × 1° grid) consisted of proglacial lakes, showed obvious lake-area expansion~~, while in~~. Conversely, some regions of Eastern Tibetan Mountains and Hengduan Shan, ~~the~~where unconnected glacial lakes occupied ~~about~~ over half of the total lake area in each grid, exhibited stability or a slight reduction~~.~~ in lake area. Our results demonstrate that proglacial lakes are a main contributor to recent lake evolution in HMA, accounting for 62.87% (56.67 ~~-~~ km^2) of the total area increase. Proglacial lakes in the Himalaya ranges alone accounted for 36.27% (32.70 ~~-~~ km^2) of the total area increase. Regional geographic variability of debris cover, together with trends in warming and precipitation over the past few decades, largely explain the current distribution of ~~supra~~ supraglacial and proglacial lake area across HMA. The Hi-MAG database is available at~~:~~ https://doi.org/10.5281/zenodo.4275164 (Chen et al., 2020~~),~~), and

it can be used for studies ~~on~~of the complex interactions between ~~glacier~~glaciers, climate, and glacial lakes, and GLOFs, potential downstream risks, and water resources.

1 Introduction

High Mountain Asia (HMA~~)~~), consisting of the whole Tibetan Plateau and adjacent mountain ranges such as ~~Himalaya~~the Himalayas, Karakoram, and Pamirs, ~~covers~~contains the largest area of mountainous glaciers ~~globally~~in the world. Atmospheric warming has resulted in widespread glacier retreat and downwasting in many mountain ranges of ~~the~~ HMA (Bolch et al., 2012; Brun et al., 2017), which ~~favor~~favors the formation and development of a large ~~amount~~number of glacial lakes~~, yet~~. However, glacial lakes have been incompletely documented ~~at~~over small time intervals. Glacial lake development varies according to climatic, cryospheric, and lake-specific conditions, ~~such as~~ including whether the basin geometry ~~that~~ is ~~either~~ connected to glaciers ~~or unconnected~~, and the length of ~~the~~ lake/glacier contact (Zhao et al., 2018).

~~Many~~There have been many previously published ~~researches have~~ studies devoted to ~~the~~mapping glacial lakes ~~mapping with remotely sensed~~using remote sensing data over ~~the~~ different regions of HMA. Some works ~~mainly focus~~have focused on ~~the investigation of~~investigating the development of relatively large glacial lakes. Rounce et al. ~~identified 131 glacial lakes in Nepal in 2015 that are greater than 0.1 km^2~~ (Rounce et al., 2017)~~.~~ identified 131 ~~Li et al. compiled an inventory of~~ glacial lakes ~~(≥0.01~~ in Nepal in 2015 that had an area greater than 0.1 km^2. Li et al. ~~) with a spatial resolution of 30 m in the Karakoram mountains~~ (Li et al., 2020)~~.~~ compiled an inventory ~~Aggarwal et al. shared a new dataset~~ of glacial ~~and high-altitude~~ lakes ~~that have an area > (≥~~0.01 km^2) with a spatial resolution of 30 m in the Karakoram mountains. Aggarwal et al. ~~for Sikkim, Eastern Himalaya from 1972–2015~~ (Aggarwal et al., 2017)~~. Ukita et al. constructed a glacial lake inventory of Bhutan in the Himalaya from the period 2006–2010 based on high-resolution PRISM and AVNIR-2 data from ALOS. Considering small lakes present less of a GLOF risk. They set 0.01 km^2 as the minimum lake size~~ shared a new dataset of glacial and high-altitude lakes having an area >0.01 km^2 for Sikkim, Eastern Himalaya in the period 1972–2015. Ukita et al. (Ukita et al., 2011)~~. Ashraf et al. used Landsat-7 ETM+ images for the 2000–2001 period to delineate glacial lakes greater than 0.02 km^2 in the Hindukush–Karakoram–Himalaya region of Pakistan~~ constructed a glacial lake inventory of Bhutan in the Himalayas for the period 2006–2010 based on high-resolution Panchromatic Remote-sensing Instrument for Stereo Mapping (PRISM) and Advanced Visible and Near Infrared Radiometer type 2 (AVNIR-2) data from Advanced Land Observing Satellite (ALOS). Considering small lakes represent less of a GLOF risk, they set 0.01 km^2 as the minimum lake size. Ashraf et al. (Ashraf et al., 2012)~~.~~ used Landsat-7 ETM+ images for the 2000–2001 period to delineate glacial lakes greater than 0.02 km^2 in the Hindukush–Karakoram–Himalaya region of Pakistan.

Because small glacial lakes ~~experience~~are highly variable in their shape, location, and occurrence~~,~~ and ~~were~~are clearly sensitive to the warming climate and glacier wastage, a growing number of scholars have ~~paied~~been paying attention to ~~the~~their abundance ~~of small glacial lakes.~~. Salerno et al. ~~provided a complete mapping of glacial lakes (including lake size less than 0.001 km^2) and debris-covered glaciers with 10-m spatial resolution in the Mount Everest region in 2008~~ (Salerno et al., 2012)~~.~~ provided a complete mapping of ~~Wang et al. utilized Landsat TM/ETM+ images for the years 1990, 2000 and 2010 to map~~ glacial lakes ~~with area more~~(including lake size less than 0.~~002~~001 km^2) and debris-covered glaciers with a 10-m spatial resolution in the Mount Everest region in 2008. Wang et al. ~~Tien Shan Mountains~~ (Wang et al., 2013)~~. Luo et al. examined glacial lake changes (lake area >0.0036 km^2) for the entire western Nyainqentanglha range for the five periods between 1976 and 2018 using multi-temporal Landsat images~~ utilized Landsat TM/ETM+ images for the years 1990, 2000,

and 2010 to map glacial lakes with areas greater than 0.002 km^2 in the Tien Shan Mountains. Luo et al. (Luo et al., 2020)~~.~~ examined glacial lake changes (lake area >0.0036 km^2) for the entire western Nyainqêntanglha range for five periods between 1976 and 2018 using multi-temporal Landsat images. The International Centre for Integrated Mountain Development ~~(ICIMOD) provided~~provided comprehensive information about the glacial lakes (greater than or equal to 0.003 km^2) of five major river basins of the Hindu Kush Himalaya ~~(HKH) using~~using Landsat images ~~for the year~~from 2005 (Sudan et al., 2018)~~. Nie et al. mapped the distribution of glacial lakes across the entire Himalaya in the year of 2015 using a total of 348 Landsat images at 30 m resolution. They set the minimum mapping unit to 0.0081 km^2~~. Nie et al. (Nie et al., 2017)~~. Zhang et al. presented a database of glacial lakes larger than 0.003 km^2 in the Third Pole for the years ~1990, 2000, and 2010~~ mapped the distribution of glacial lakes across the entire Himalaya in 2015 using ~~a total of~~ 348 Landsat images at 30-m resolution. They set the minimum mapping unit to 0.0081 km^2. Zhang et al. (Zhang et al., 2015) presented a database of glacial lakes larger than 0.003 km^2 in the Third Pole for the years 1990, 2000, and 2010.

All of these ~~researches greatly~~studies significantly help to fill the data gap ~~of glacial lakes~~ relating to information about glacial lakes in the HMA region. At the global scale, Pekel et al. (Pekel et al., 2016) ~~used millions of Landsat satellite images to record global surface water over the past 32 years at 30 metre resolution~~ used millions of Landsat satellite images to record global surface water over the past 32 years at 30-m resolution, and many large and visible glacial lakes were also included. More recently, Shugar et al. ~~mapped glacial lakes with areas >0.05 km^2 around the world using 254,795 satellite images from 1990 to 2018~~ (Shugar et al., 2020)~~. Wang et al. developed a~~ mapped glacial ~~lake inventory (~~lakes with ~~size of larger than~~ areas >0.~~0054~~ 05 km^2~~) across~~ around the ~~High Mountain Asia at two time periods (1990 and 2018)~~world using ~~manual mapping on 30 m Landsat~~254,795 satellite images from 1990 to 2018. Wang et al. (Wang et al., 2020b)~~.~~ developed an inventory of glacial lake with areas greater than 0.0054 km^2 across HMA at two time points (1990 and 2018) using manual mapping with 30 m Landsat images. They ~~firstly~~ were the first to introduce a glacial lake inventory at such a large~~-~~scale, and the data shared will ~~be served~~serve as a baseline for ~~the~~ further studies related to water~~-~~ resource assessment ~~or~~and glacier ~~hazard risk.~~ hazards.

In summary, a homogeneous, annually resolved inventory and analysis of the spatial and temporal extent of different types of glacial lakes over the entire HMA ~~has~~region is still ~~been~~ lacking. ~~We~~In this study, we developed ~~a~~an HMA ~~Glacial Lake Inventory~~glacial lake inventory (Hi-MAG) database to characterize the annual coverage of glacial lakes from 2008 to 2017 at 30~~-~~m resolution. A total of 40,481 Landsat scenes were processed using the Google Earth Engine (GEE) cloud~~-~~computing platform to delineate glacial lakes (located within 10~~-~~km ~~from~~of the nearest glacier terminus) larger than nine (e.g., 3~~×~~ × 3) pixels (0.0081~~-~~km^2) (Nie et al., 2017).

Lakes were manually classified into four categories according to their position relative to the parent glacier or their formation mechanisms (Fig.~~-~~A1~~):~~). Category (i~~)~~), proglacial lakes, are usually connected to the glacier tongue and dammed by glacier ice~~,~~ or unconsolidated or ice-cemented moraines (a mixture of ice, snow, rock, debris ~~and,~~ clay, etc~~.), proglacial.~~). Proglacial lakes are located next to the glacier terminus and receive melt water directly from their mother glaciers~~;~~. Category (ii~~)~~), supraglacial lakes ~~this is where~~, are ponds that form in depressions on low-sloping parts of the surface of a melting glacier and are dammed by ice or the end-moraine or stagnating glacier snout~~;~~. Category (iii~~)~~), unconnected glacial lakes, ~~which~~ are ~~glacial lakes~~ not currently directly connected to their parent glaciers ~~at the present time~~ but ~~which,~~they may to some extent~~, may~~ be fed by at least one of the glaciers located in the basin ~~and~~. They may ~~have been~~ (but not necessarily ~~are~~)) have recently detached from ice contact due to glacial recession. Although not directly connected with the parent glaciers, these glacial lakes are also ~~the~~an outcome of glacier melting in response to atmospheric warming~~, they~~. They can

supply fresh water to major river systems of the HMA region, and their changes have significant scientific and ~~socio-economic~~socioeconomic implications (Nie et al., 2017; Song et al., 2016)~~; and~~. Finally, category (iv~~)~~), ice-marginal lakes, ~~these lakes~~ are generally distributed on one side of the glacier tongue, ~~which means~~meaning that the lake is dammed by the glacier ice on this side~~. While~~, while on the other side, it is bounded by a lateral moraine. With the increase of atmospheric warming and accelerated melting of ~~glacier~~glaciers, some glacier ~~tributary~~tributaries gradually ~~detaches~~detach from a main trunk glacier. ~~The detached location~~These detachment locations, where glacier melting has been particularly intense, is in some ~~case is~~cases also likely to form ice-marginal lakes. We note that such ice-marginal lakes are very common in some parts of the world (e.g., Alaska) but are not common in HMA (Armstrong and Anderson, 2020; Capps et al., 2011)~~ but are not common in HMA. Besides~~. Additionally, purely glacier-dammed lakes are formed by the advance of glaciers and dammed by almost pure glacier ice. Although the dam composition and structure is slightly different between ~~the~~ proglacial lakes and glacier-dammed lakes, because they are all located in the front of the glacier tongue and driven by the mother glacier, in the process of appending attributed information to each glacial lake, glacier-dammed lakes were merged into ~~class of~~the proglacial lakes category.

Every lake was cross-checked manually for its boundary and attribution. We defined an uncertainty of 1 pixel for the detected glacial lake boundaries~~,~~ and calculated the error in the lake area ~~error~~ for the whole HMA region. We also assessed the inventory for climatic and geomorphological influences on lake distribution across HMA.

2 Study area and data

2.1 Study area

The ~~term~~ HMA region refers to a broad high-altitude region in South and Central Asia that covers the whole Tibetan Plateau and adjacent mountain ranges, including the Eastern Hindu Kush, Western Himalaya, Eastern Himalaya, Central Himalaya, Karakoram, Western Pamir, Pamir Alay, Northern/Western Tien Shan, Dzhungarsky Alatau, Western Kunlun Shan, ~~Nyainqentanglha~~Nyainqêntanglha, Gangdise Mountains, Hengduan Shan, Tibetan Interior Mountains, Tanggula Shan, Eastern Tibetan Mountains, Qilian Shan, Eastern Kunlun Shan, Altun Shan, Eastern Tien Shan, Central Tien Shan, and Eastern Pamir (~~Fig.~~ Figs. 1 and ~~Fig.~~ 6a). It extends from 26°N to 45°N and from 67°E to 105°E, and the altitude of the plateau is about 4500~~-~~ m on average (Baumann et al., 2009). ~~It's~~It is made up of alternating mountains, valleys, and rivers, and the terrain is fragmented, showing a decreasing terrain from ~~Northwest~~northwest to ~~Southeast.~~ southeast. The HMA region has a series of ~~East-West mountains~~east–west mountain ranges that occupy most of the area. Among these, Tanggula Shan lies in the central part of ~~the~~ HMA, with an altitude of over 6000~~-~~ m. The ~~height~~heights of the fifteen highest mountains in the Himalayas are ~~more~~greater than 8000~~-~~ m, while the peaks of the mountains in the northern plateau are ~~more~~greater than 6500~~-~~ m. The ~~North-South mountains~~north–south mountain ranges are mainly distributed in the southeast of the plateau and near the Hengduan Mountain area. These two groups of mountains constitute the geomorphic framework and control the basic pattern of the plateau landform. Continuous and discontinuous permafrost have developed on the higher land and north~~-~~facing slopes.

The HMA region is the source of several of Asia's major rivers, including the Yellow, Yangtze, Indus, Ganges, Brahmaputra, Irrawaddy, Salween, and Mekong. They play a crucial role in downstream hydrology and water availability in Asia (Immerzeel and Bierkens, 2010). Most glaciers in the Tibetan Plateau are retreating, except for the Western Kunlun (Neckel et al., 2014; Kääb et al., 2015) and the Karakoram, where a slight mass gain is occurring (Bolch et al., 2012;

Gardner et al., 2013). Moreover, glaciers in different mountain ranges show contrasting patterns. Local factors (e.g., exposure, topography, and debris coverage) may partly account for these differences, but the spatial and temporal heterogeneity of both the climate and degree of climate change may be the main reason. Glacial lakes are formed and ~~developed~~develop temporally with the retreat or thinning of glaciers and are directly or indirectly fed by glacier meltwater~~, they~~. They are located within 10 km ~~from~~of the nearest glacier terminus (Wang et al., 2013; Zhang et al., 2015).

The HMA climate is under the combined and ~~competitive~~competing influences of the East Asian and South Asian monsoons and of the westerlies (Schiemann et al., 2009). This unique geographical position produces an azonal plateau climate characterized by strong solar radiation, low air temperatures, large daily temperature variations, and small differences between annual mean temperatures (Yao et al., 2012). The annual mean temperature is 1.6 °C, with the lowest temperature of −1 °C to −7 °C occurring in January and the highest temperature of 7 °C to 15°C occurring in July. The cumulative annual precipitation is about 413.6 mm ~~a year.~~.

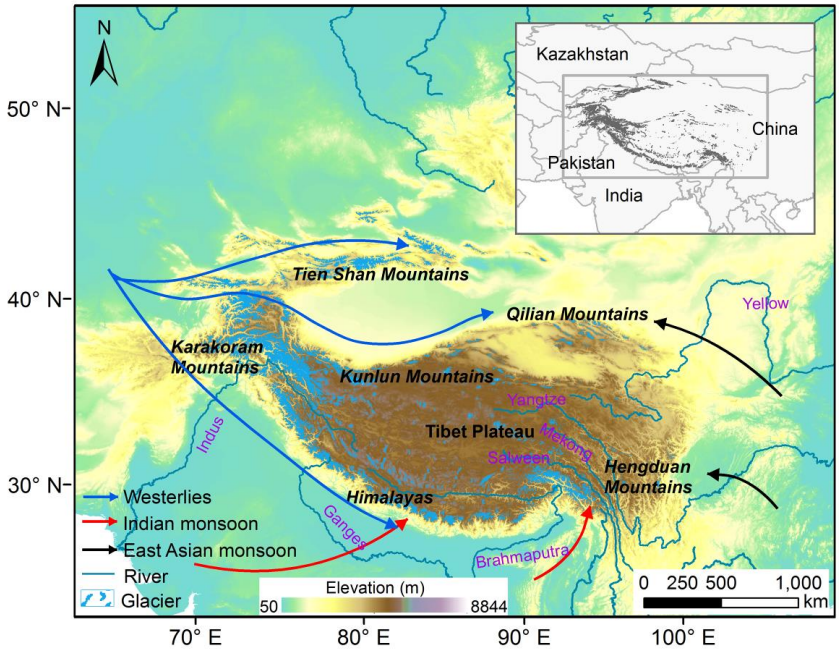

Fig. 1. ~~**The location**~~ Location of the ~~**High Mountain**~~HMA region ~~**of Asia (HMA).**~~ Glacier outlines from the Randolph Glacier Inventory (RGI v5.0), the Second Chinese Glacier Inventory (CGI2~~)~~), and the Glacier Area Mapping for Discharge from the Asian Mountains (GAMDAM) glacier inventory are drawn in ~~sky~~ blue.

2.2 Dataset

A total of 40,481 satellite images, including Landsat 5 TM imagery during 2008 ~~to~~ 2011, Landsat 7 ETM+ imagery in 2012, and Landsat 8 OLI during the period 2013 ~~to~~ 2017, were available in GEE and were used to produce the annual glacial lake maps over the entire HMA (Fig. 2). Here, when Landsat 5 or 8 data were available, Landsat 7 ETM+ imagery with Scan Line Corrector (SLC)-off gaps were generally excluded due to ~~their~~the artefacts induced by the slatted appearance of the original images, but these were exclusively used for the glacial lake mapping in 2012 since no other Landsat data were acquired that year. For the years before 2008, all the available Landsat 5 TM data in each year (e.g., 2004, 2005, 2006, and 2007) do not fully cover the HMA region.

The SLC-off condition of Landsat ETM+ introduces artefacts because the slatted appearance of the original images is occasionally carried into the glacial lake map in 2012. Techniques to fill the SLC-off gaps exist, but these create artificial values that will result in false detections of water (Chen et al., 2011). Considering the strong spatial and temporal variability of glacial lakes ~~like~~such as supraglacial lakes, techniques ~~which~~that merge data from one or more SLC-off fill scenes for generation of a gap-free image require careful use, even when using the thousands of Landsat ETM+ images. It is noted that water mapping using multi-temporal time~~ ~~~~-~~~~series images at large scales usually ~~avoided~~avoids the use of such techniques (Mueller et al., 2016). Therefore, Landsat 7 ETM+ data with intensive slatted appearance ~~is~~are not ~~really a good and~~ suitable~~ data~~ for the classification of numerous of glacial lakes. In this study, because the only useable data source for ~~the year of~~ 2012 ~~is~~was from Landsat 7 ETM+, to ensure continuity of annual data from 2008 to 2017, we ~~have tried~~applied our best efforts to ~~manually extract~~manual extraction of the glacial lakes from the 2012 ETM+ images ~~as accurately as~~with the highest possible~~.~~ accuracy.

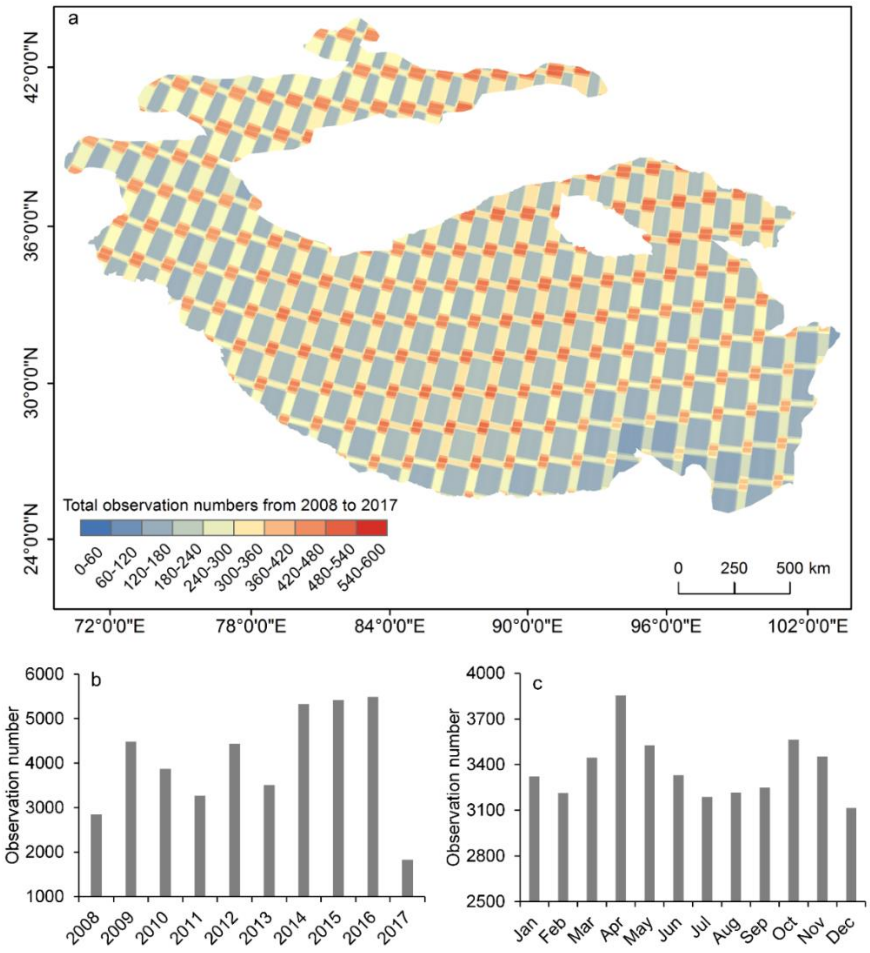

Fig.~~ ~~2. (a) The distribution of total observation numbers from all GEE Landsat scenes, along with these numbers broken down by **(b)** year and **(c)** month.

3 Methods

3.1 Satellite imagery selection strategy

~~To~~One effective solution to reduce the influence of seasonal lake fluctuations ~~for~~on the mapping~~, one effective solution~~ is to map glacial lakes and measure their long-term changes during stable seasons when the lake extents are minimally affected by meteorological conditions and glacier runoff. ~~Here~~Here, based on analyses of the mapping times of glacial lakes in different regions, the selected time series of Landsat data were generally from July to November ~~based on the analyses of mapping time of glacial lakes in the different regions.~~. During this period of each year, the Landsat imagery featured ~~less~~lower perennial snow coverage. ~~Change in~~ Following glacier runoff and precipitation, the area of a glacial lake is ~~minor and has a~~ large and changes in this area ~~following the glacier runoff and precipitation~~will be small (Nie et al., 2017; Chen et al., 2017; Zhang et al., 2015). ~~The~~These lakes may also ~~reached~~reach their maximum extent around the end of the glacier ablation season (June to August) (Gardelle et al., 2013; Liu et al., 2014)~~-~~, except in ~~the central~~Central and ~~eastern~~Eastern Himalaya, where peak ablation extends into post-monsoon September and October. In monsoon-affected areas such as Nepal and Bhutan, monsoon cloud cover ~~in~~from July to mid-September means that ~~most of those areas are covered by~~ clear-sky images can mostly only be obtained from late September to November. ~~Southeast~~The southeastern Tibet ~~regions are~~region is problematic, not only because the observation season is short, but as a result of abundant cloud cover, which is formed by the warm and humid airflow raised by the topography (Zhang et al., 2020; Umesh et al., 2018; Qiao et al., 2016).

As the most highly variable glacial lakes in the study area, supraglacial lakes change preferentially in the year, showing an increase in area during the pre-monsoon, and rising to ~~the~~their peak area in the early monsoon (June to July) (Miles et al., 2017a; Miles et al., 2017b). Although the selected image seasons are slightly different due to the meteorological conditions in different regions, they all comply with the same criterion that ~~lake area~~the lakes were in clear-sky images ~~and has~~having small snow coverage. This ~~will ensure~~ensured the initial reliability of the mapping of glacial lakes through the GEE cloud~~-~~computing platform. If no valid observations ~~can~~could be obtained, then the optimal mapping time ~~needs~~needed to be broaden during the whole year.

To further increase data availability, and also as the basis for data selection in the periods beyond the optimum mapping time, we set two criteria for the selection of imagery with valid observations over the potential glacial lake area by using the cloud~~-~~score functions in GEE, including (i) cloud cover ~~is~~being less than 20% in the 10~~-~~km buffer around each glacier ~~outlines~~outline of a Landsat scene, or (ii) less than 20% cloud cover for the entire scene. The cloud~~-~~score functions in GEE may ~~face a big challenge to detect~~have significant difficulty in detecting clouds in mountain headwaters with high snow and ice cover, where large amounts of snow and ice are likely to be identified as clouds. However, in this study, it ~~is a~~was considered better to use much stricter criteria to filter out ~~more~~a larger number of images with lots of cloud or cloud-lookalike objects (snow/ice) ~~and~~to finally ~~choose~~select only images with good observations.

3.2 Extraction of glacial lake outlines

For the development of ~~HMA Glacial Lake Inventory (~~the Hi-MAG~~)~~ database, we applied a systematic glacial lake detection method that ~~combined~~comprised two steps ~~from:~~ initial glacial lake extraction and ~~subsequently~~subsequent manual refinement of these lake mapping results. The main procedures for glacial lake mapping using Landsat data, as shown in Fig. 3, are ~~(Fig. 3):~~as follows. (i) ~~the~~The Landsat top~~-~~of~~-~~atmosphere data were clipped according to the extent of the glacier buffers and assembled into a time-series dataset~~:~~. (ii) ~~poor~~ Poor-quality observations were identified~~——~~these

included areas affected by cloud, cloud shadow, topographic shadow, and SLC-off gaps. Here, we used the Fmask routine (Zhu and Woodcock, 2012) to detect the clouds and cloud shadows in an imagery. Fmask has the advantage of being able to process a large number of images in a computationally efficient way. Topographic shadows are located in the areas where the sunlight is blocked, generally. Generally, on the dark side of the high mountains, theirthe surface gradients are great, and the terrain reliefs are small. Therefore, topographic shadows were masked using the slopes (larger than 10°) and shaded relief values (less than 0.25) calculated from SRTMShuttle Radar Topography Mission (SRTM) data (Li and Sheng, 2012; Quincey et al., 2007). This will removeremoves a considerable number of mountain shadows that have the similar spectral reflectance withas water bodies. However, the SRTM DEMdigital elevation model (DEM) was generated in 2000, which is different from the acquisition time of the Landsat images used for the glacial lake mapping in this study, the. The derived slopes and shaded relief cannot therefore fully represent the conditions on the date a given Landsat scene iswas acquired. As a consequence, some lakes that have grown at steep glacier tonguetongues may be masked, and some mountain shadows that interfere with the mapping results of glacial lakes from GEE still remain, leading to the fact that glacial lakes in the steep areas are omitted, and residual shadows are misclassified as glacial lakes. As for the SLC-off gaps in the ETM+ images, lakes out ofoutside the gaps werewill be accurately classified, but if glacial lakes they are covered by gaps, then they will be misclassified. Errors caused by striped gaps ofin Landsat ETM+ data were manually corrected using additional high-quality scenes duringacross the whole year with the assistance of images from adjacent years. (iii) theThe modified Normalized Difference Water Indexnormalized difference water index (MNDWI) was calculated (Xu, 2006);. (iv) theThe potential glacial lake areas were extracted by applying an adaptive MNDWI threshold (Li and Sheng, 2012). To define a glacial lake in the image, theThe minimum number of water pixels wasused to define a glacial lake in an image is inconsistent in different studies. For example, Zhang et al.,. (2015) set the smallest detectable glacial lakes in the Third Pole ofas being larger than 0.0027 km^2 (three connected pixels) using the Landsat TM/ETM+ data. Nie et al.,. (2017) selected 0.0081 km^2 (nine connected pixels) as the minimum mapping unit to map glacial lakes in the HimalayaHimalayas. Other studies have set the minimum threshold areas as 0.001km^2 (Salerno et al., 2012), 0.002km^2 (Wang et al., 2013), 0.0036km^2 (Luo et al., 2020), 0.0054km^2 (Wang et al., 2020b), of 0.01km^2 (Li et al., 2020) for the identification of glacial lakes and analysis of their spatial and temporal variations.. A smaller minimum mapping unit will detect more glacial lakes, however. However, the uncertainty itthis brings iswill also be larger than large lakesusing a larger threshold at the same resolution (Salerno et al., 2012). Our results demonstrate that a lake area covering fewer than nine water pixels will have an area error of largergreater than 50% (Please see the Section 4). Given the area uncertainty in the areas of glacial lakes and the spatial resolution of Landsat data, in this study, glacial lakes larger than nine pixels (≥ 0.0081 km^2) were considered as the minimum mapping unit; and. (v) manualManual inspection and refinement of individual glacial lake werelake was conducted, and the related attributionattributions were added for each lake.

Based on the automated processing, nearly 60% of glacial lakes in each year can be correctly classified, of. Of the other lakes that were not properly classified, 30% were missed and 10% were misclassified. For such a large-scale area that is characterized by various and complex climatic, geological, and terrain conditions, this classification method is simple but effective, the. The results are also reasonable since it providesthey provide very low commission errors. To ensure the quality of the inventory, strict quality control was conducted to visually inspect and correct the mapping errors after the automated processing using GEE. False lake features, mainly identified as mountain shadows and river segments, were manually removed by overlapping mapped lake shorelines on the source Landsat imagery and higher-resolution imagery in Google Earth. For missingSome glacial lakes, such as some lakes may be covered by ice and clouds for years, grow at steep

glacier tongues, ~~and lakes~~or show heterogeneous reflectance with the surrounding backgrounds~~, the lake~~. For these missing glacial lakes, their boundaries were edited further using ArcGIS. Furthermore, a cross-check and modification was conducted for each glacial lake based on the lake ~~-~~-mapping results in conjunction with multi-temporal Landsat imagery. Here, all the Landsat imagery that was used for the inspection ~~were~~was downloaded manually from the United States Geological Survey (USGS) Earth Explorer website ~~(https://earthexplorer.usgs.gov/). Outputs per~~ (https://earthexplorer.usgs.gov/). The outputs for each lake polygon include ~~the~~ information about the lake type, elevation, Euclidian distance to the nearest glacier terminus, area, and perimeter. ~~Noted~~Note that if there ~~are~~was more than one suitable satellite ~~images~~image in a year, the image with the ~~least~~lowest cloud cover ~~will be~~was selected for the calculation of the area and perimeter of a given lake. ~~Meanwhile, each~~Each mountain range was characterized individually by utilizing the mountain boundary shapefile in ~~High Mountain Asia (geo.uzh.ch/~tbolch/data/regions_hma_v03.zip).~~HMA (http://geo.uzh.ch/~tbolch/data/regions_hma_v03.zip).

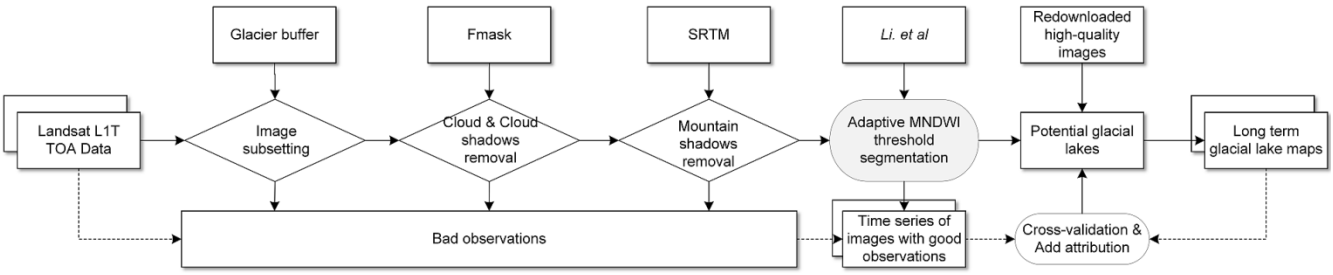

Fig. ~~-~~ **3.** Diagram of the glacial lake mapping workflow.

3.3 Yearly lake area changes calculations

Based on the final generated lake inventory data, we used the slope of a linear regression of the lake area (over the grid ~~cell~~cells of 1~~°×°~~ × 1°) versus mapping year to qualify the yearly changes in lake area ~~changes~~ during the study period. The ~~approach to~~ change analysis ~~was predicted using a~~ used the Theil ~~-~~-Sen estimator, which chooses the median slope ~~among~~of all the derived fitted lines,~~,~~ can effectively represent long-term area changes due to its robustness for ~~the~~ trend detection and its insensitivity to outliers~~, it~~. It is also useful for the elimination of ~~the effect~~effects arising from differences in ~~the~~ sensor performance for the mapping of glacial lakes (Sen, 1968; Song et al., 2018).

Although all the ~~lake~~lakes were manually checked and edited, due to the limitation of available images and other factors, the conditions ~~of~~for glacial lake mapping ~~are~~were not perfectly consistent for each year. For example, the image dates ~~are~~were not consistent across the whole HMA region because of atmospheric disturbances, and there were also ~~the~~ influences from varying lake characteristics, image quality (Bhardwaj et al., 2015; Thompson et al., 2012), ice and ~~shadow~~shadows that obscured the lakes, which all contributed to ~~the~~ detection errors in the lake extent and their annual variation. Generally, these errors ~~are~~were objective and acceptable as a result of the nature of the limited remote sensing data. For this study, because we used ~~long~~ time ~~-~~-series ~~(10~~data covering a period of ten years~~) data~~ for the estimation of annual changes in lake area ~~change~~, and also because the errors only ~~accounts~~account for a small proportion of the total glacial lake area for each year, the errors in the observed lake area caused by ~~the~~these different effects do not ~~apparently~~appear to affect the ~~trend~~ trends in the statistical results. ~~For the glacial lake area time series in each 1°×1°grid, we applied~~ In addition to the Theil ~~-~~-Sen estimator ~~to smooth the annual time series of data and derive the slope (annual~~

~~change) of the trend. A,~~ a Mann~~–~~Kendall trend test was used to detect and further confirm the statistical confidence ~~by~~of the linear regression results~~. All~~, and all the estimated trends were found to fall within the 90% confidence intervals. The upper and lower change estimates ~~that satisfy~~satisfying the 90% confidence interval for the slope were also derived over the whole HMA region (Fig.~~-~~ A2).

4 Cross-validation and uncertainty ~~estimate~~estimates

Accuracy assessment of the mapping results is difficult due to the lack of field measurements of glacial lakes in ~~the~~ continental-scale ~~area like~~ areas such as HMA. To obtain ~~the~~ quality~~–~~controlled data, the glacial lake ~~vector~~vectors over the entire HMA for the years from 2008 to 2017 ~~has been~~were rechecked and reedited individually through dynamic cross-validation by ten trained experts~~, which is~~. This was a time~~–~~consuming process but ~~are~~was essential ~~to maximize~~for maximizing the quality of ~~glacial lake change detection~~the data.

~~For~~A key factor influencing the estimation of the uncertainty ~~of~~in the glacial lake area~~, a key influence factor~~ measurements is the spatial resolution of the satellite data. ~~–~~In this study, the uncertainty of the glacial lake area was estimated as an error of ±1 ~~pixels~~pixel on either side of the delineated lake boundary. The percentage error of the area determinations~~,~~ A_{er} , A_{er} , is then ~~is~~ proportional to the sensor resolution and is given by (Krumwiede et al., 2014)~~:~~

域代码

~~$A_{er} = 100 \cdot (n^{1/2} \cdot m) / A_{gl}$ (1)~~

~~Where~~ $A_{er} = 100 \cdot (n^{1/2} \cdot m) / A_{gl}$, (1)

域代码

where n ~~refers to~~is the number of pixels on the boundary of a glacial lake, as approximated by the ratio of the perimeter length and the spatial resolution, m is the area of a pixel in the Landsat image (m^2), A_{gl} is the lake area (m^2) and the factor 100 ~~is there~~converts the value to ~~convert to~~a percentage.

Assuming an uncertainty of 1 pixel for the detected glacial lake boundaries, we calculated the systematic errors for the whole HMA region ~~(~~, and the results are shown in Fig.~~-~~ 4~~).~~. For the ~~year~~years between 2008 and 2017, the area uncertainty of each glacial lake generally ranged from 0.30% to 50%, with the mean value falling around ~~the~~ 17~~%,~~% and the standard deviation around 11% (Fig.~~-~~ 4a). The maximum and mean ~~value~~values of area uncertainty for the glacial lakes in 2010 ~~are~~were the lowest, while for ~~the year of~~ 2016, the corresponding statistics ~~are~~were the highest~~, this~~. This can be attributed to ~~the~~a number of different factors. The maximum ~~of~~in the area uncertainty of glacial lakes is related ~~with~~to the shape and size of a certain lake ~~(~~, as can be seen from ~~equation~~ Equation (1~~)), but~~). However, its mean value is equal to the sum of the area uncertainties of each glacial lake divided by the total number, which ~~depend~~depends on the total number of glacial lakes in a given year, ~~and also~~as well as the shape and area of each lake. ~~Besides~~Furthermore, a close relationship can be found between the area uncertainties and ~~the~~ sizes of the glacial lakes (Fig.~~-~~ 4b). Most of the large glacial lakes (area ≥ ≥ 0.~~04km~~^{2}04 km^2) have ~~the~~a mean area uncertainty of about 7%. ~~This~~These systematic errors were more significant for the small-sized glacial lakes. We measured glacial ~~lake~~lakes down to 0.0081~~-~~ km^2 (nine pixels in Landsat imagery), where systematic errors calculated by ~~equation~~ Equation (1) were ~50%.

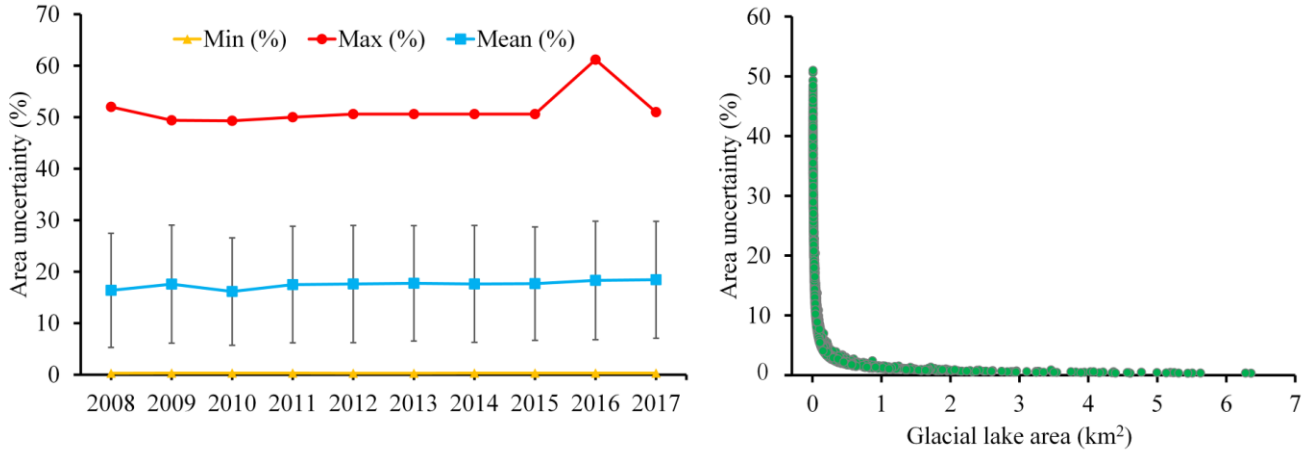

Fig. 4. (a) Statistics ~~of area~~ relating to the uncertainty (%) in the measured areas of glacial lakes for the years from 2008 to 2017. **(b)** Relationship between the area uncertainties and the areas of all the glacial lakes in HMA in 2017.

5 Results

5.1 Distribution of various types and sizes of glacial lakes

The area coverage of glacial lakes increased by 90.14 km^2 ~~between~~in the period 2008–2017, a 6.90% increase relative to 2008 (1305.59 ~~±~~ ± 213.99 km^2) (Fig. 5a). A Theil–Sen regression fit to all the data showed a mean expansion rate of 12 ~~km^2 a^{-1}~~ km^2 a^{-1} for the ~~10~~ten-year record ~~(~~, as shown in Fig. 5a~~)~~. Meanwhile, the estimated changes in glacial lake number from 2008 (12,593 lakes) to 2017 (15,348 lakes) showed an average increase of 306 lakes a^{-1}. The steeper percentage increase in ~~lake~~the number of lakes (22.33%) compared to ~~a~~the slower ~~area~~ expansion of their area (8.79%) based on their linear fit trends ~~showed~~shows that many small glacial lakes formed over this ~~decade~~period. The number of lakes increased most rapidly in areas beyond 4400 m above ~~4400 m~~ sea level (a.s.l~~.~~.), especially ~~above~~beyond 5300 m (Fig. 5b). The increase ~~of~~in proglacial lakes was concentrated above 4900 m (Fig. 5c). Unconnected glacial lakes grew very slightly in total area below 4400 m (Fig. 5d~~),~~) but increased notably more at higher elevations. Glaciers are retreating and thinning at ever-higher elevations (Nie et al., 2017), causing the formation of new supraglacial lakes at high ~~elevation,~~ elevations, the expansion of existing ice-contact lakes, and the detachment of glaciers from some lakes.

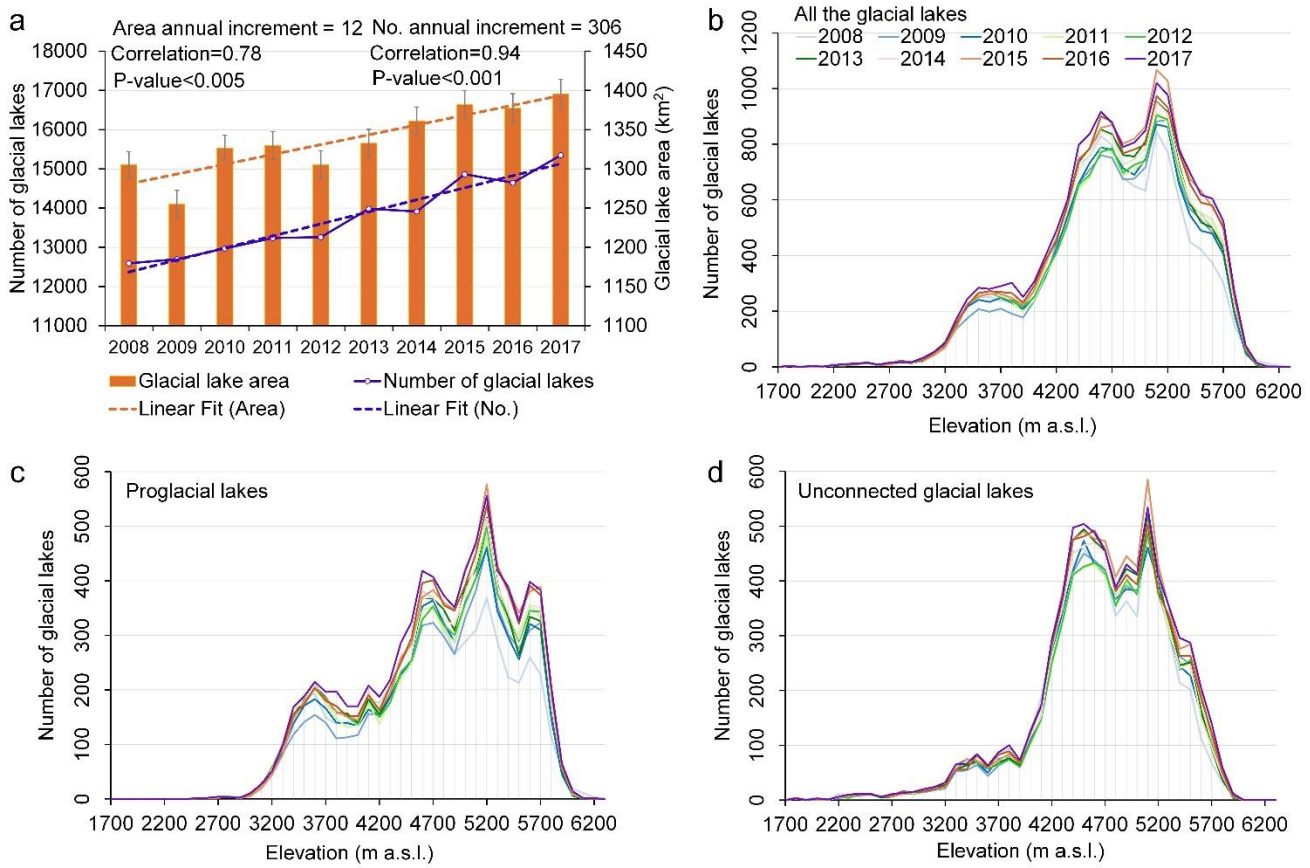

Fig. 5. ~~**Annual glacial lake number**~~Numbers and ~~**area,**~~total areas of glacial lakes for different years. **(a)** Total number and area of glacial lakes for HMA ~~between~~in the period 2008–2017. The annual increment is the slope of the trend of annual lake area and number. Altitudinal distribution (100-m bin sizes) of lake numbers for **(b)** all glacial lakes, **(c)** proglacial lakes, and **(d)** unconnected glacial lakes.

Annual changes in glacial lakes were further analyzed spatially using a 1°~~×~~° × 1° grid over 22 mountain regions (Fig. 6a) using Theil–Sen regression analysis. An analysis ~~on~~of the mountain-wide lake area loss/gain from 2008 to 2017 was conducted (Table A1). Negative or undiscernible changes in glacial lake area were observed in the Eastern Tien Shan, Eastern Hindu Kush, Hengduan Shan, and Eastern Tibetan Mountains (Fig. 6b), thus reducing the otherwise overall increasing glacial lake area in HMA. The Eastern Hindu Kush lost 2.8 km^2 of lake area (Table A1), with ~~the~~a negative area change (~~(~~−0.43 ~~km^2 a~~ $km^2\ a^{-1}$) near 35°N, 73°E. Glacial lakes in ~~Nyainqentanglha,~~Nyainqêntanglha and Gangdise Mountains exhibited area loss and gain in ~~some~~different regions. In contrast, Central and Eastern Himalaya~~,~~ and Central Tien Shan showed rapid increases in lake area ~~increases~~. Between 2008 and 2017, Central Himalaya's glacial lake area increased by 27.09 km^2 (Table A1), exhibiting both a high density of 47 glacial lakes per 100 km^2 in 2017 (Fig. A3) and rapid growth, +0.94 ~~km^2 a~~ $km^2\ a^{-1}$, in lake area due to retreat and thinning of debris-covered glaciers (Song et al., 2016). Moderate area gains occurred along most of the Western Kunlun and Tanggula Shan, e.g., +0.38 ~~km^2 a~~ $km^2\ a^{-1}$ in Tanggula Shan. ~~Glacial lake area~~The areas of glacial lakes in Pamir Alay, Eastern Pamir, and Eastern Kunlun Shan ~~was~~were spatially and temporally invariant across the whole observation record.

We found that glacial lakes exhibited different expansion trends for different lake types and supraglacial and ice-marginal lakes have relative few coverage areas comparing with proglacial and unconnected lakes (Fig. 6b and Fig. 6c). In

the ~~Nyainqentanglha~~Nyainqêntanglha and Central Himalaya, around half of the glacial lake area consisted of proglacial lakes, where most growth ~~occurs~~occurred. In the negative lake growth (shrinkage) regions of the Eastern Tibetan Mountains and Hengduan Shan, ~~the~~ unconnected glacial lakes were dominantly occupied. As the interaction with ~~the~~a glacier gradually ~~weakened~~weakens, part of the water source supplied by ~~glaciers~~that glacier is reduced~~. Also,~~, and when combined with the effects from atmospheric warming and a decrease ~~of~~in precipitation, this means that regions mainly ~~consist~~consisting of unconnected glacial lakes show ~~the~~a trend of decreasing ~~trend in~~ area. Proglacial lakes contributed approximately 62.87% (56.67 km^2) ~~of~~to the total area increase over HMA (~~Table~~ Tables A1 and A2). Proglacial lakes in ~~the~~ Central Himalaya, Eastern Himalaya, and Western Himalaya~~,~~ accounted for 36.27% (32.70 km^2) of the total area increase. In general, proglacial lakes are ~~a~~the main contributor to recent lake evolution in HMA.

We also noted the large area growth of lakes occurred in areas with a relatively large proportion of small glacial lakes, and this was mainly due to the rapid growth of existing lakes and ~~new lake~~the formation of new lakes (Fig. 6d). For example, in some areas of Central and Eastern Himalaya~~, Nyainqentanglha~~ and Nyainqêntanglha that have large annual ~~increase~~increases in lake area (~~higher~~greater than 0.23 ~~km^{2}a^{-1}~~ km^2 a^{-1}), glacial lakes with a size of less than 0.16 km^2 occupied more than 30% of the total area (Table A3). ~~Especially for the region in Nyainqentanglha~~In particular, in Nyainqêntanglha, the area of small glacial lakes (≤0.16 km^2) ~~even accounts~~accounted for 69.47% of the total area.

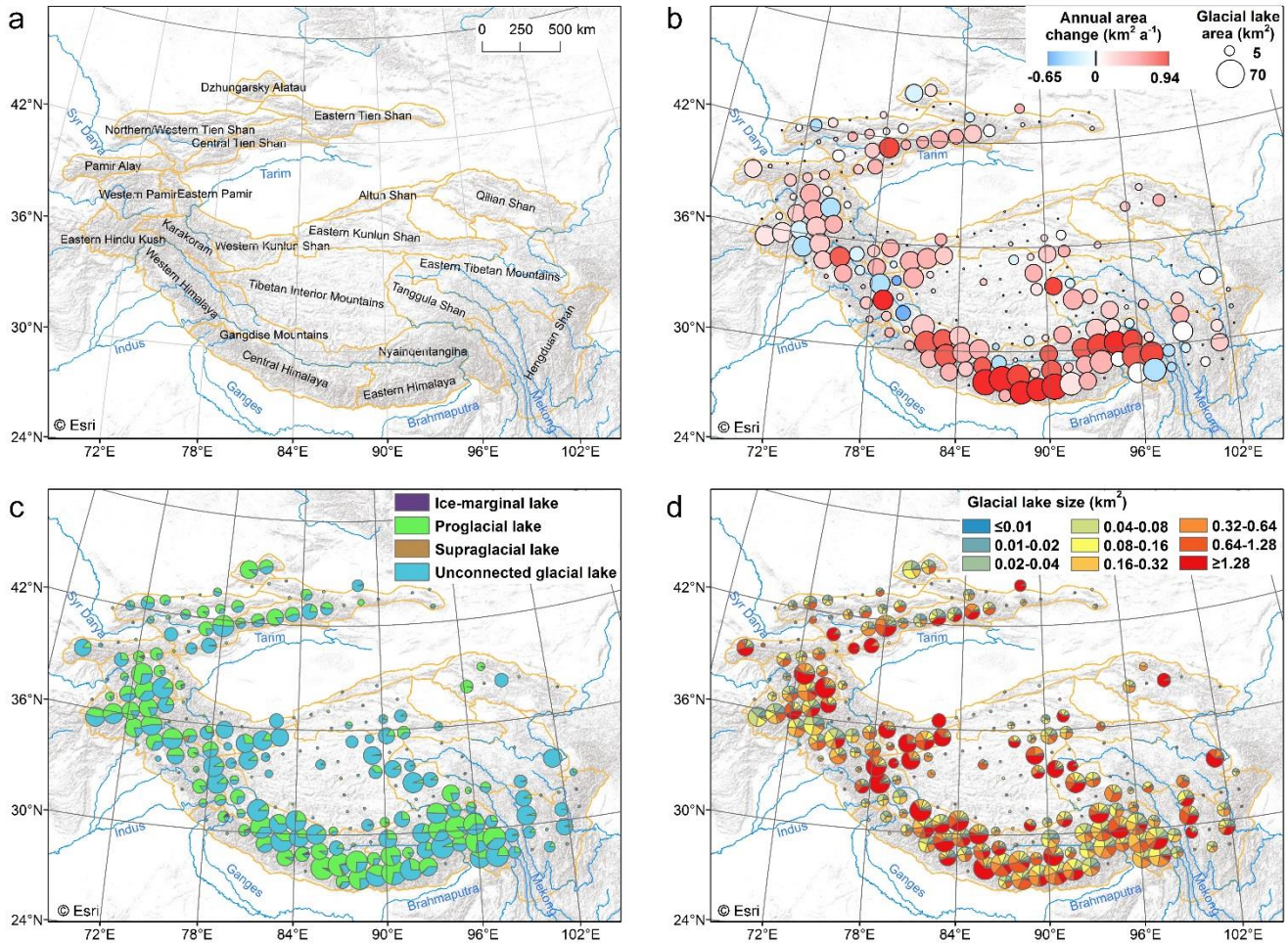

Fig. 6. Glacial lake area changes and area distribution. **(a)** Geographic coverage of mountain ranges in HMA. **(b)** Annual rate of change in lake area (2008–2017) on a 1°×° × 1° grid. The sizesizes of the circle forcircles represent the total glacial lake area in 2017. **(c)** Proportional areas of four types of glacial lakes in 2017. **(d)** AreaAreas of different sizes of glacial lakes in 2017. The terrain basemap is sourced from Esri (© Esri).).

5.2 Influencing factors of current distribution of glacial lakes

To explore potential factors that have potentially influenced the glacial lake distribution across HMA, we focus on proglacial and supraglacial lakes, for which the changes are closely related with glaciers and expansion is most rapid. Proglacial lakes frequently develop from the enlargement and coalescence of one or more supraglacial lakes (Thakuri et al., 2016; Umesh et al., 2018). Proglacial and supraglacial lake development from 2008 to 2017 is significantly correlated towith initial lake area in 2008 (R= = 0.82, Table A4); larger ice-contact proglacial lakes imply a larger water body in contact with the calving front of the glacier, and more rapid retreat (Truffer and Motyka, 2016; King et al., 2019).

For the years before 2008, the year-round Landsat 5 TM data in many years do not fully cover the HMA region. In this study, we constructed the inventory over a ten-year time period, which. This is shorter than typical glacier response times, which start from a minimum of 10ten years for short, steep glaciers, to over 150 years for long, debris-covered glaciers (Scherler et al., 2011). Hence, lake expansion is not expected to coupleto be coupled with short-term climate trends, particularly for debris-covered glaciers (Umesh et al., 2018). In the inclusion of mass balance forcing of glacial lake changes, the same questions about the response times also occur. Hence, rather than focus on the short term evolution of lake expansion, we investigated ifwhether the climate and other factors have influenced the overall distribution of lake area, as observed in 2017.

To investigate the factors influencing the predominance of proglacial and supraglacial lakes, geomorphic, topographic, and climate parameters were correlated with lake area over a 1°×° × 1° grid, and these were aggregated (taking the mean or summedsum) for HMA regions. A statistically significant positive correlation exists between lake area and debris-covered glacial area (after Scherler et al. 2018) across HMA (R= = 0.36, Table A4), confirming the predominance of pro proglacial and supraglacial lakes forming on debris-covered glacier tongues (Nie et al., 2017). Correlations and significance levels strengthen if the Karakoram is excluded (Table A5). The Karakoram is known as an anomaly of positive glacier mass balances and glacier advances (Gardelle et al., 2012) and also has an anomalously small area of proglacial lakes. Glacier length (RGI-Consortium, 2017) and debris cover are strongly correlated (R= = 0.85, Table A4), reflecting abundant debris on most large, low-gradient valley glacier tongues in HMA; in turn, there is a statistically significant direct correlation between glacier length and lake area (R= = 0.32, Table A4), as these tongues provide the ideal conditions for the coalescence of supraglacial ponds and formation of large proglacial lakes (Nie et al., 2017; Richardson and Reynolds, 2000)., Glaciers are generally longest and most heavily debris covered in the Hindu Kush Himalaya region (Figs. 7a and 7b).

Some regions have comparable amounts of large debris-covered glaciers but substantial differences in total lake area and area-growth rates (for example, Central Himalaya compared to Central Tian Shan or Western Pamir, Table A5).). Regional differences in multi-decadal climate trends could play a role in this observation, with Nyainqentanglha,Nyainqêntanglha and the Central and Eastern Himalayan regions all being characterized by rapid warming and decreased precipitation since 1979 (Fig. Figs. 7c and Fig. 7d), favoring negative glacial mass balances (Brun et al., 2017). This plausibly explains why the lake area is typically larger in these regions relative to adjacent regions further to the west and north (e.g. Western Himalaya) despite often similar glacier characteristics (in terms of debris cover and glacier length) (Figs. 7e and 7f).

~~Further~~Furthermore, there is very little debris-covered area but rapid warming in Eastern Himalaya, where proglacial lakes are abundant (Fig. 7f). These results emphasize that the distribution of ~~supra~~supraglacial and proglacial lakes across HMA ~~are~~is primarily associated with the presence of large debris-covered glaciers, but regional variability in warming and precipitation trends over the past few decades have likely also had some influence (Shugar and Clague, 2011; Zhao et al., 2019; Umesh et al., 2018; Scherler et al., 2018)~~.~~. These results are consistent with previous findings at regional scales, ~~that~~which have demonstrated a rapid expansion of proglacial lakes on debris-covered glaciers, with expansion in the upstream direction demonstrated to occur primarily through a process of subsidence at ~~of~~ the lake-contact debris-covered glacier tongue (Harrison et al., 2018; Song et al., 2016; Song et al., 2017a).

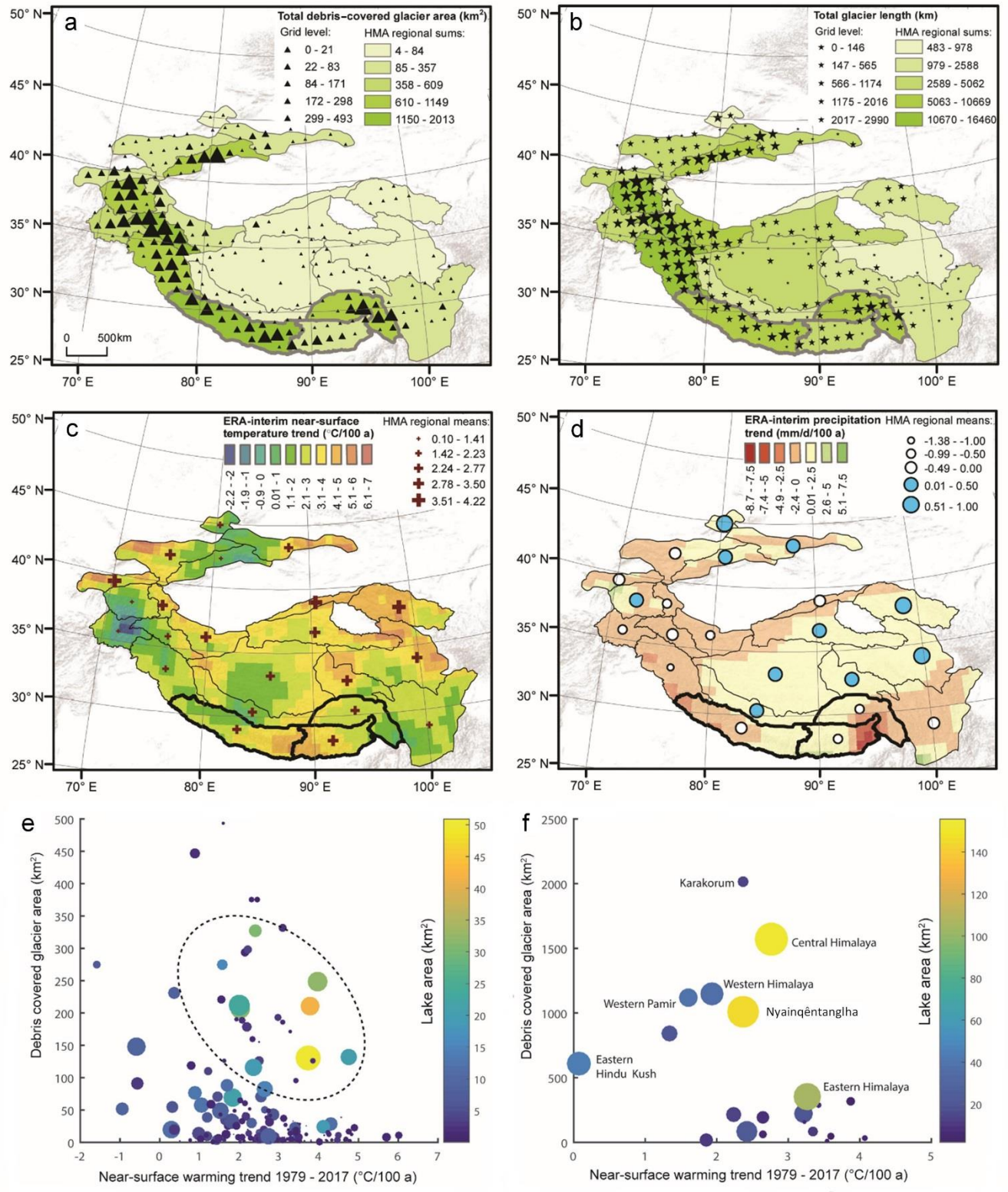

Fig. 7. Geomorphic and climatic influences on lake distribution. **(a)** Debris-covered area and **(b)** glacier length aggregated on a 1°×° × 1° grid. Linear trends in **(c)** temperature and **(d)** precipitation calculated for 1979–2017 from ERA-Interim, including aggregated means over HMA regions. Relationship between total debris-covered area, near-surface temperature warming, and proglacial and supraglacial lake area of 2017 in **(e)** 1°×° × 1° grid tiles and **(f)** HMA regions. Some regions

discussed in the text are ~~labelled~~labeled. The lake coverage is high in areas of both rapid warming and high debris cover (~~E~~e, dashed ellipse). Dot sizes are proportional to lake number. See Table A4 for details on data sources.

6 Discussions

6.1 Comparison with other lake datasets

We compared our dataset with that of Wang et al.~~,~~. (2020) for the closest period (2017 from the Hi-MAG database and 2018 from Wang et al., 2020) over the spatial extent of our HMA region. The differences in the total number and area of lakes between these two ~~dataset~~datasets are 6206 and 223.97 km^2, respectively. We also found that 2077 glacial lakes with a total area of 178.77km^2 in our Hi-MAG dataset were not detected by Wang et al. The main reasons for the missed glacial lakes in Hi-MAG are because the interference of some bad observations (cloud or snow), glacial ~~lake~~lakes that have dried up or outburst, or were located in the middle of the river.

To test the spatial correlation of the distributions of the glacial lakes ~~distribution~~ in the two datasets, we compared the ~~statistics in~~numbers of glacial ~~lake number~~lakes and ~~area~~their areas aggregated on a 0.1~~°×°~~ × 0.1° grid for the HMA regions. The results for the total glacial lake area, areas ~~for glacial lakes larger than 0.04km^2, and number for~~of glacial lakes larger than 0.~~04km^2~~04 km^2, and the number of glacial lakes larger than 0.04 km^2 are ~~depicted~~shown in Fig. A4. A clear and strong correlation can be observed for all the statistics between the Hi-MAG dataset and the glacial lake data of Wang et al. Most of the points ~~being~~are distributed around the 1:1 line, which shows that there is great consistency ~~in~~between the ~~results.~~ two sets of data.

~~In order to~~To quantitatively and systematically evaluate the accuracy of our ~~product~~data, we implemented ~~a~~ stratified random sampling (Song et al., 2017b; Stehman, 2012)~~, where~~, in which the glacial lakes were divided into four strata. The sample sizes ~~are~~were the spatial resolution (30 m) of the data, and the strata ~~are~~were designed as: C0W0~~.~~ indicates that both the results are non-glacial lakes; C1W1~~. non~~ indicates a non-glacial lake in the present data and a glacial lake ~~for Chen's and~~ in Wang's data; C1W0 indicates a glacial lake ~~for Wang's; C1W0.~~ in the present data and a non-glacial lake ~~for Chen's and non-glacial lake for~~in Wang's~~;~~ data; and C1W1~~. Both the~~ indicates that both results are glacial lakes.

A total of ~~4,000~~4000 points were randomly selected, as shown in Fig. A5. The ~~sample~~ number of samples for C1W1 and C1W0 ~~are~~were 1300 and 700, respectively, ~~which is~~and these numbers have almost the same ratio as that between the total areas for the two strata (1450.50 km^2 vs 732.77 km^2). Because of the approximate total area with C1W0, we also randomly selected 700 samples from stratum C0W1. The ~~rest~~remaining 1300 samples ~~are~~were from C0W0. Every validation sample was visually examined using Landsat imagery and higher-resolution imagery in Google Earth. Sample pixels were interpreted by a regional glacial lake mapping expert, and ambiguous samples were cross-validated by a second observer. If a sample ~~is~~was difficult to interpret, it was marked as ambiguous ~~sample~~ and excluded ~~for~~from the accuracy assessment. The sample number estimates were produced for each of the four strata (Table A6), and these strata totals were then summed to obtain the total accuracy.

For the 1300 ~~pixel~~ samples that were considered by both datasets to be non-glacial lakes ~~by both datasets~~, after the pixel-by-pixel verification, 1215 were found to indeed be non-glacial lakes, while 37 were ~~the~~ missed glacial lakes. In ~~contrary~~contrast, 1260 out of the 1300 ~~pixels belongs~~samples belonged to the class of glacial ~~lake~~lakes, and 25 ~~pixels~~ were misclassified as glacial lakes by ~~the two~~both inventories. A total of 307 error pixels were found in the results ~~from~~of Wang et al., ~~constitute~~constituting about half of the total validation number. For the glacial lakes identified only by our inventory,

678 out of 700 were ~~corrected~~correctly classified. Our results yielded high overall classification accuracy (88%), user's accuracy (97%), and producer's accuracy (82%) for glacial lake classification using Landsat data.

The Hi-MAG dataset was also compared with other Landsat-based lake inventories (Nie et al., 2017; Pekel et al., 2016; Zhang et al., 2015)~~.~~. The number of lakes in Hi-MAG ~~lake number~~ was found to be 7268 higher and the area was 644.26 ~~-~~ km^2 ~~higher~~greater than the estimation for the Tibetan Plateau (Zhang et al., 2015). The largest ~~discrepancy is~~ discrepancies were found in the Gangdise, Himalaya, and ~~Nyainqentanglha~~Nyainqêntanglha Mountains in 2010. Across the Himalaya region, we found 476.09 ~~-~~ km^2 of glacial lakes, 4.57% more than previous estimates in 2015 (Nie et al., 2017). In addition, we qualitatively compared the lake ~~extent~~extents between the publicly available high-resolution Global Surface Water (GSW) dataset (Pekel et al., 2016) and our Hi-MAG database summed by mountain range in 2015. ~~GSW data can be accessed at https://global-surface-water.appspot.com/download.~~ For the sake of a reliable comparative analysis, lake polygons in the Hi-MAG dataset were converted into ~~the~~a grid format, and glacial lakes in the GSW were further extracted using the range of glacier buffer (10 km). Hi-MAG detected more glacial lakes in the Himalaya region, Eastern Hindu Kush, and Tien Shan, and fewer in Eastern Pamir and Western Kunlun Shan. Fig. ~~-~~ A6 illustrates the differences between our Hi-MAG glacial lake results and the GSW-derived lake area for the whole HMA region.

The glacial lake area observed in our lake dataset in the Eastern Pamir and Western Kunlun Mountains does not conform to the mapped surface water in the GSW for these sub-regions. While there are numerous glacial lakes from an open water perspective, actually part of them are river segments. Additionally, the Himalaya, Eastern Hindu Kush, and some other Tien Shan areas host thousands of glacial lakes that are not readily observable in the GSW ~~product~~dataset. Large discrepancies in mountainous glacial lake estimates preclude a significant consistency between GSW and our Hi-MAG lake data over the HMA region. The region with the highest consistency between GSW and Hi-MAG product is interior Tibet. There is little agreement for Tien Shan, where the weather is rainy and snowy in the region above 3000 ~~-~~ m, and large ~~amounts~~quantities of ancient glacial deposits have ~~been~~ accumulated. Here, glacial lakes are ~~featured~~characterized by small ~~size,~~sizes, and due to the influence of their source glaciers and lake beds, as well as the water depth and sediment inflow, glacial lakes appear to have heterogeneous reflectance in the ~~image.~~images. Errors could exist in datasets produced by automated classification, but, as noted, we also ~~did a~~conducted detailed manual editing, so we were not relying exclusively on automatic classification. The Karakoram ~~regions seem~~region seems to have fewer glacial lakes in our estimate, owing to the overestimation of surface water on debris ~~-~~ covered glaciers in the GSW dataset.

The ~~little~~low agreement between our Hi-MAG glacial ~~lakes~~ lake data and the GSW data is mainly due to its lack of systematic glacial lake ~~inventories~~inventory and mapping capabilities. The lake dynamics and differing climate contexts within HMA may also lead to inconsistencies between the sub-regions. Hi-MAG might have made better use of the optimum satellite imaging season to map glacial lakes, potentially resulting in more complete mapping by avoiding conditions —such as periods of lake ice —that may confound mapping.

6.2 Known issues and planned improvements

There are several important issues and limitations to the datasets produced and the methods used within this study that are important to highlight to potential users. (i) Bodies of water smaller than nine connected pixels (e.g., 1 ~~x~~ × 9 pixels or 3 ~~x~~ × 3 pixels, corresponding to 30 ~~x~~ × 270 ~~-~~ m or 90 ~~x~~ × 90 ~~-~~ m, respectively~~),~~) and those obscured by frozen water surface ~~and~~or loose moraines or hidden by terrain shadows were not included. Broken floating ice or isolated ~~moraine~~moraines that ~~stand~~stood in open water for some ~~times~~time were mapped. Supraglacial lakes such as melt ponds developed on the surface

of glaciers present particular challenges because of their small size and highly dynamic properties. Most supraglacial lakes are transient or seasonal, or at least fluctuate seasonally, as they commonly drain and may refill~~, but in~~. In fact, this short-duration seasonal water is in general more ~~generally is~~ likely to be underestimated because of temporal discontinuities in the archive and gaps caused by persistent cloud cover. (ii) The spatial and temporal information reported in the Landsat dataset used in this study complements that acquired in the past. Nevertheless, the biggest limitation to glacial lake mapping from these data are undoubtedly the geographic and temporal discontinuities of the Landsat archive itself. Historical data over the entire HMA before 2008 can be recovered partly from the Landsat 4 TM/MSS, Landsat 5 TM, Landsat 7 ETM+, and partly from SPOT, and other satellite systems, etc., although data access is not always at the full, free, and open level of Landsat. In this regard, ASTER is freely accessible and has a higher resolution than Landsat, but ~~the~~its temporal coverage is very limited in most of HMA. Other Landsat-like moderate resolution multi-spectral sources could be also used to improve and extend the temporal sampling. For example, the European Space Agency's Sentinel 2a satellite launched in 2015 and provides optical imagery at 10 ~~-~~m resolution (Wang et al., 2020a; Yu et al., 2020), which will benefit future research combing all available satellite observations with GEE cloud computing power would make long-term monitoring of changes to HMA's glacial lakes and inland waters possible.

7 Data availability

The Hi-MAG database is distributed under the Creative Commons Attribution 4.0 License. The data can be downloaded from the data repository Zenodo at https://doi.org/10.5281/zenodo.4275164 (Chen et al., 2020).

8 Conclusions

In conclusion, the Hi-MAG dataset and others have ~~turned to~~used Earth observation satellite data, especially Landsat imagery, to provide a more consistent delineation of large-scale glacial lake changes. Some remote-sensed glacial lake mapping methods have enabled local-scale area estimation or spatial representation of lake extent and change. Such methods result in relatively good performance for lake areas that remain clear and show homogeneous reflectance in the image, but do not allow for continental-scale ~~glacial lake~~ mapping of glacial lakes that have spectral interference from ~~the~~ other objects such as glaciers, snow, clouds, turbidity, and the sedimentation characteristics of the glacial lake itself, or the atmospheric interference and terrain effects. Automated methods for the extraction of glacial lakes over ~~the~~ large-scale areas ~~are~~have been further developed in ~~our~~this work. However, visual interpretation and manual editing is still an effective way to ensure ~~the~~ high accuracy of lake inventories and append attributed information for further analysis. Based on an error of ±1 ~~pixels~~pixel on the lake boundary, the area uncertainty of each glacial lake ~~ranged~~ranges from 0.30% to 50% for the ~~year~~years between 2008 and 2017, and ~~the~~there is a mean area uncertainty of 17% in the entire HMA region.

Mapping of glacial lakes across the Tibetan Plateau and adjoining ranges reveals a complex pattern of lake occurrence and growth/shrinkage. During the past ten years, 2755 glacial lakes with a total area of 90.14 km^2 were increased in the HMA region. Proglacial lakes contributed 62.87% of that increase. We found that most ~~of~~ areas in HMA have experienced rapid expansions, Central and Eastern Himalaya~~,~~ and Central Tien Shan showed the most lake area increases (up to +0.94 $km^2\ a^{-1}$). Negative area changes were observed in the Eastern Tien Shan, Eastern Hindu Kush, Hengduan Shan, and Eastern Tibetan Mountains. The number of lakes ~~grown~~grew very rapidly above 4400 m a.s.l~~. Proglacial.~~, and proglacial lake growth is proceeding at high elevations of above 4900 m, but glacier retreat and lake disconnections are also starting to occur at higher elevations, causing the number and area of both classes to increase. At low elevations, few glaciers remain

where proglacial lakes can form, and already detached lakes lack growth mechanisms. Overall, continued growth of glacial lakes can be expected, particularly where large debris-covered tongues remain.

580 ~~This~~The freely~~ ~~downloadable, detailed Hi-MAG dataset can also be used in future studies to provide a sound and consistent basis on which to quantify critical relationships and processes in HMA, including glacier~~ ~~~~climate~~ ~~lake interactions, glacio-hydrologic models, GLOFs and potential downstream risks, and water resources.

Appendix A

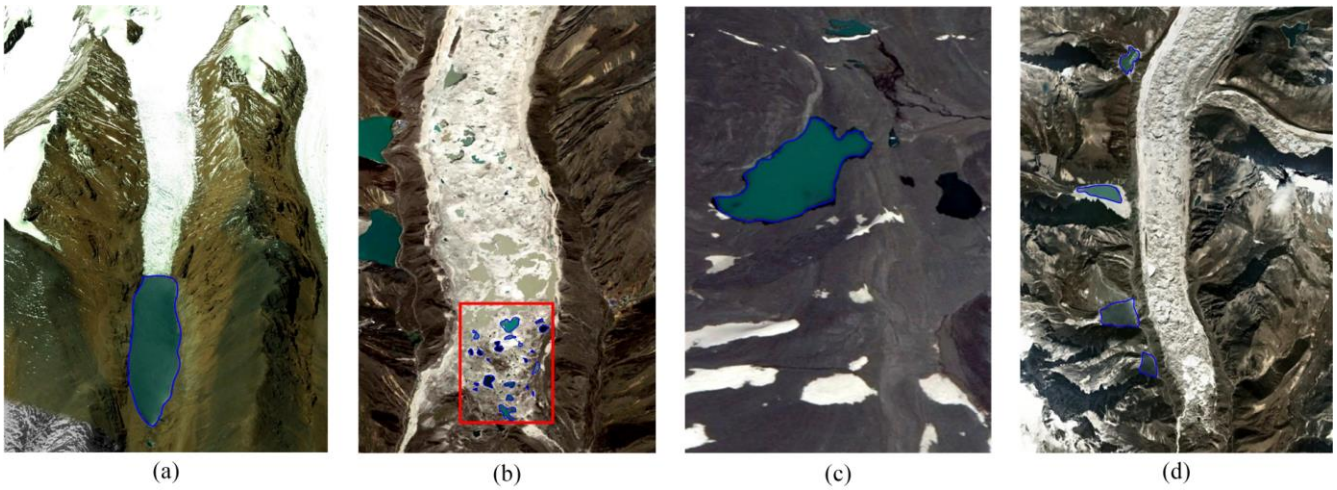

Fig. A1. Examples of the various types of glacial lake found in the HMA region: **(a)** ~~pro-glacial~~proglacial lakes, which are connected to the parent glacier and usually impounded by a debris dam (usually a moraine or ice-cored moraine); **(b)** supraglacial lakes (denoted by the red rectangle), which develop on the glacier surface; **(c)** unconnected glacial lakes; and **(d)** ice-marginal lakes that are distributed on the edge of a glacier. Background images were acquired from © Google Earth, and were ~~shot~~obtained in 2009, 2011, 2012, and 2014, respectively. Glacial lake outlines for each type are shown in blue ~~color~~.

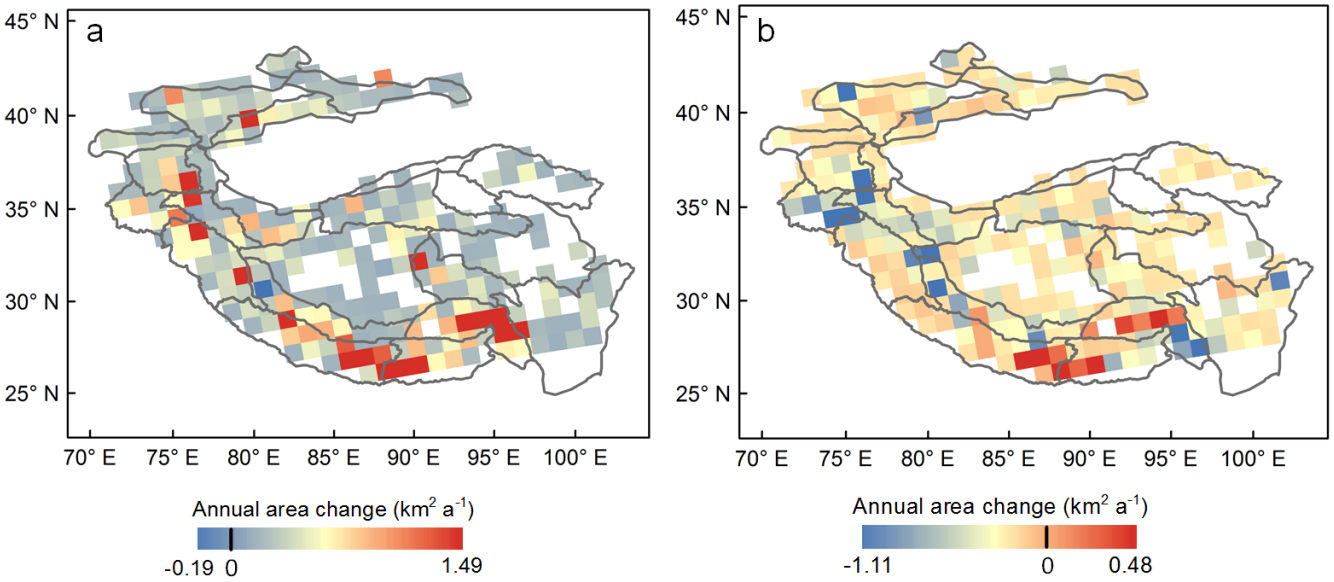

Fig. A2. Annual changes in lake area between 2008 and 2017 on a 1°~~x~~° × 1° grid. The **(a)** upper and **(b)** lower slopes represent the 90% confidence interval.

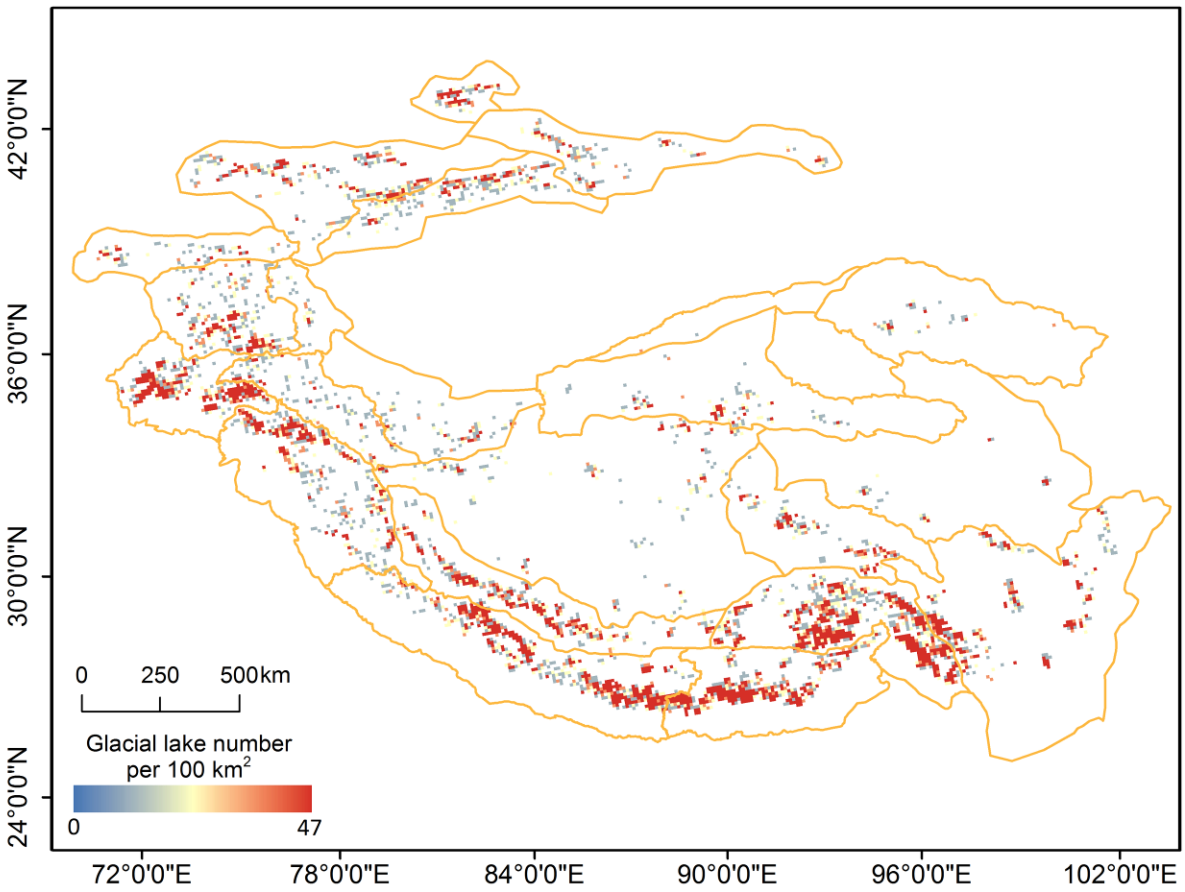

Fig. A3. Density (number per 100 km^2) distribution of glacial lakes in 2017.

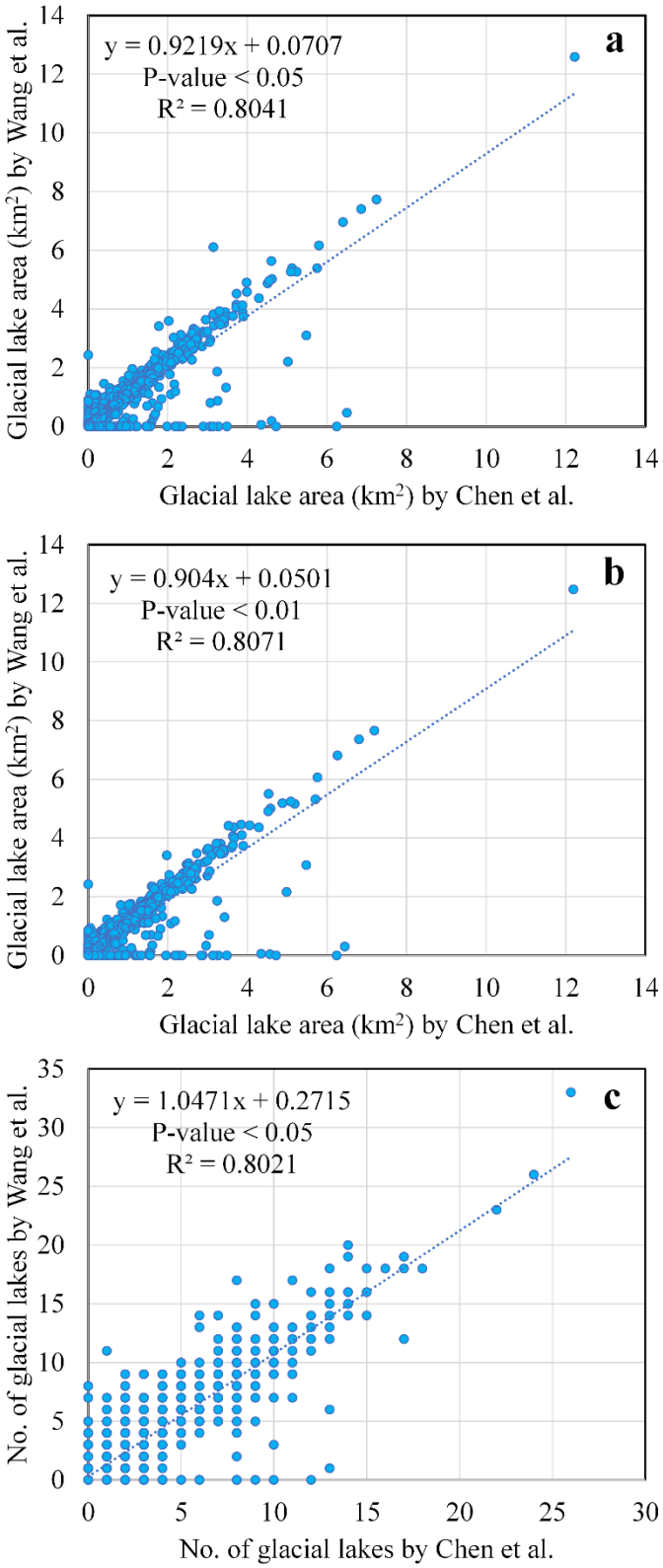

Fig. **A4.** Comparison of the results of **(a)** total glacial lake area, **(b)** areas ~~for~~of glacial lakes larger than 0.04 km^2, and **(c)** number ~~for~~of glacial lakes larger than 0.04 km^2 summed over a 0.1~~°×~~° × 0.1° grid between the Hi-MAG database and the inventory ~~by~~of Wang et al~~.,~~. (2020~~.~~).

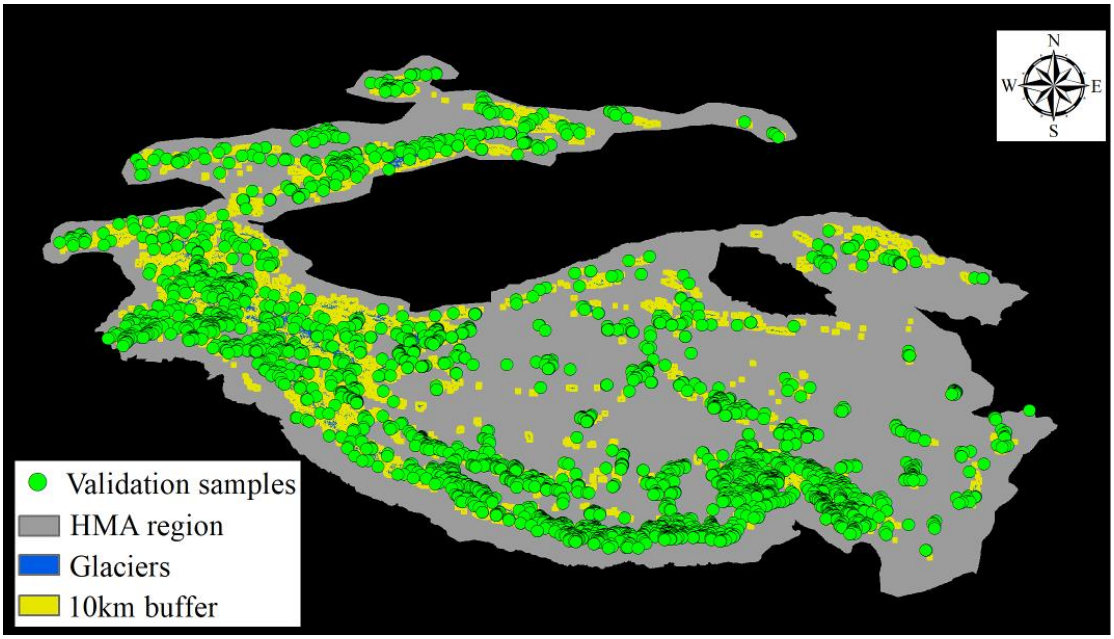

Fig. A5. Distribution of validation samples selected using stratified random sampling. Blue polygons are glacier outlines taken from the Randolph Glacier Inventory (RGI v5.0), the Second Chinese Glacier Inventory (CGI2) and the GAMDAM inventory. Yellow polygons refer to buffer ~~area~~areas within 10 km of glacier terminals.

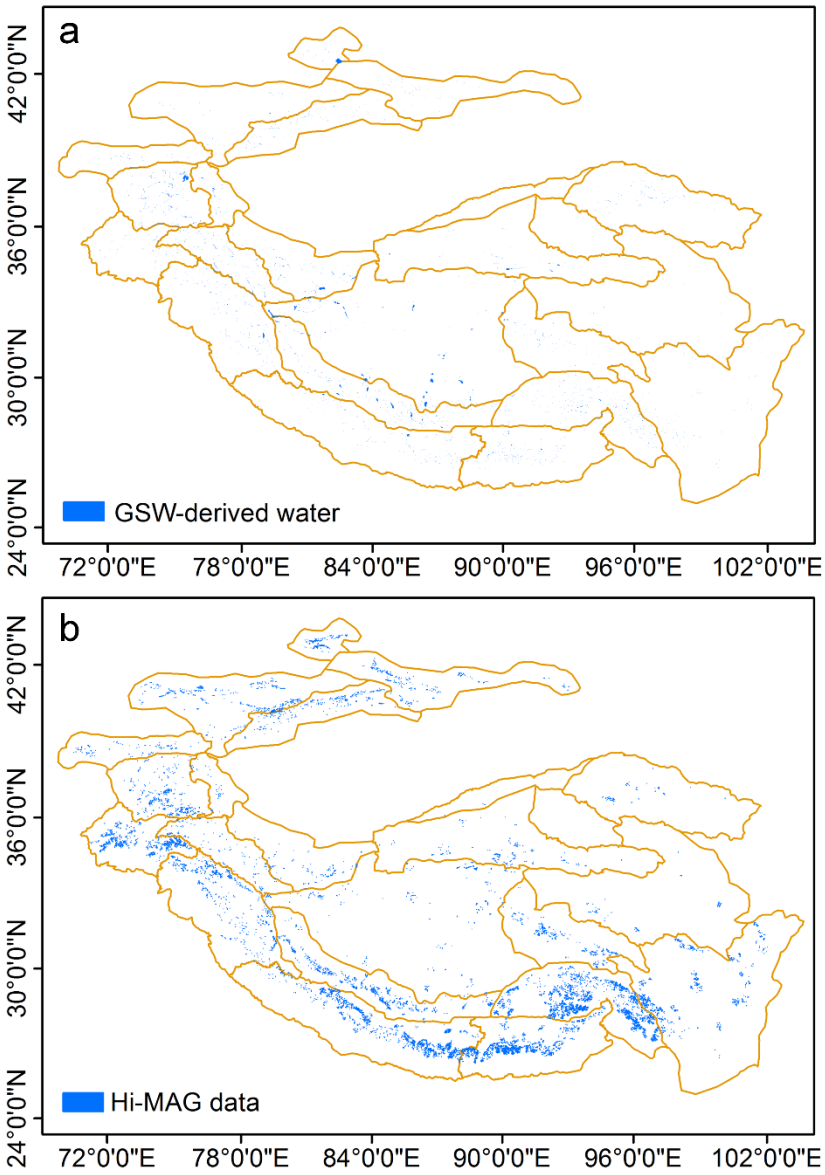

Fig. A6. Comparison of the glacial ~~lake~~lakes measured in the global maps ~~of~~as in the **(a)** Pekel et al. (2016) and **(b)** our Hi-MAG data.

Table A1. Mountain-wide glacial lake number and area per year, and total loss/gain from 2008 to 2017. The unit of area is km^2.

Mountain range	2008		2009		2010		2011		2012		2013		2014		2015		2016		2017		Total gain/loss (2008–2017)	
	No.	Area	No.	Area	No.	Area	No.	Area	No.	Area	No.	Area	No.	Area	No.	Area	No.	Area	No.	Area	No.	Area
Eastern Hindu Kush	1227	73.63	856	61.40	1113	68.91	1036	67.94	1015	59.80	1206	67.90	1179	71.30	1172	66.36	1260	65.77	1399	70.83	172	−2.80
Western Himalaya	894	77.65	856	70.23	756	71.25	747	71.38	746	68.95	779	76.00	874	82.76	823	78.33	999	79.51	1005	87.96	111	10.31
Eastern Himalaya	1634	164.12	1667	163.10	1675	166.49	1836	172.87	1859	171.67	1910	176.54	1943	174.93	2159	190.96	1954	179.09	1943	179.80	309	15.68
Central Himalaya	1312	182.54	1697	179.04	1577	188.35	1847	195.77	1782	195.56	1728	196.72	1850	198.52	2049	206.80	2096	206.41	2182	209.63	870	27.09
Karakoram	167	18.89	214	16.78	206	17.91	159	14.90	152	13.55	182	14.76	163	15.41	182	17.02	250	18.26	219	18.60	52	−0.29
Western Pamir	481	75.53	486	77.64	526	83.27	548	80.86	495	79.17	537	79.32	550	81.20	557	83.96	570	81.76	624	75.82	143	0.29
Eastern Pamir	38	5.06	45	5.69	48	5.81	43	4.99	56	5.75	50	5.43	50	5.26	49	5.65	58	5.66	56	5.81	18	0.75
Pamir Alay	124	10.82	79	9.76	100	10.93	132	11.79	129	11.60	127	11.74	128	11.66	137	11.79	130	11.54	131	12.10	7	1.28
Northern/Western Tien Shan	474	36.16	358	37.20	499	36.87	541	41.71	522	36.04	518	36.98	551	46.06	530	38.28	512	37.38	626	40.91	152	4.75
Central Tien Shan	307	29.19	241	29.43	305	32.65	334	35.44	340	35.41	335	32.36	333	36.07	337	35.51	441	35.97	471	36.69	164	7.50
Eastern Tien Shan	247	15.83	230	17.24	241	15.99	245	15.64	251	15.75	259	16.15	250	16.07	297	17.31	241	17.99	245	18.31	−2	2.48
Western Kunlun Shan	112	40.27	134	38.30	121	36.92	119	41.41	111	39.84	136	37.09	108	37.62	120	41.62	126	40.54	132	44.71	20	4.44
Eastern Kunlun Shan	180	11.92	193	12.83	265	20.62	237	16.46	232	15.74	246	15.90	244	16.72	290	18.49	255	17.95	248	16.90	68	4.98
Gangdise Mountains	852	99.15	908	96.46	848	104.24	886	96.88	961	102.48	895	95.75	954	96.28	991	94.64	1053	96.37	1116	99.83	264	0.68
Hengduan Shan	909	62.25	1077	64.70	967	65.38	867	61.29	927	62.75	1064	66.53	948	63.82	1023	65.45	942	62.93	961	63.35	52	1.10
Tibetan Interior Mountains	335	52.96	308	44.76	349	47.59	334	46.42	318	46.94	334	47.73	313	46.17	335	48.12	318	44.74	315	47.97	−20	−4.99
Eastern Tibetan Mountains	57	12.74	86	13.74	86	14.39	107	15.38	84	13.65	100	14.35	93	14.93	76	13.58	85	14.53	66	13.60	9	0.86
Tanggula Shan	468	39.45	318	40.99	344	44.28	327	43.24	347	42.17	363	43.40	376	44.97	461	45.53	372	45.94	363	44.97	−105	5.52
Qilian Shan	82	7.96	78	8.67	91	9.68	77	9.23	76	9.19	85	9.36	90	10.38	86	9.90	80	9.99	67	8.97	−15	1.01
Dzhungarsky Alatau	290	13.82	218	11.57	233	11.75	272	12.60	259	12.48	269	12.68	267	12.90	205	11.80	240	12.44	264	12.80	−26	−1.02
~~Nyainqe~~~~tanglha~~Nyainqêntanglha	2401	275.33	2647	255.23	2614	272.95	2539	273.28	2594	266.60	2856	275.46	2646	277.70	2977	280.35	2660	292.24	2911	285.68	510	10.35

Table A2. Mountain-wide annual glacial lake area from 2008 to 2017 for proglacial lakes and unconnected lakes. Supraglacial and ice-marginal lakes have ~~relative~~relatively few coverage areas and are not listed ~~details~~ in the table. The unit of area is km^2. Acronyms are used to represent the ~~name~~names of mountain ranges to save space (Eastern Hindu Kush (EHK), Western Himalaya (WH), Eastern Himalaya (EH), Central Himalaya (CH), Karakoram (K), Western Pamir (WP), Eastern Pamir (EP), Pamir Alay (PA), Northern/Western Tien Shan (N/WT), Central Tien Shan (CT), Eastern Tien Shan (ET), Western Kunlun Shan (WK), Eastern Kunlun Shan (EK), Gangdise Mountains (G), Hengduan Shan (H), Tibetan Interior Mountains (TIM), Eastern Tibetan Mountains (ETM), Tanggula Shan (T), Qilian Shan (Q), Dzhungarsky Alatau (DA), Nyainqêntanglha (N)).

		EHK	WH	EH	CH	K	WP	EP	PA	N/WT	CT	ET	WK	EK	G	H	TIM	ETM	T	Q	DA	N	Total
Proglacial lakes	2008	46.71	34.58	91.45	133.06	10.99	34.07	4.56	4.13	17.77	14.52	9.12	5.15	1.58	24.01	11.40	3.59	0.76	9.73	3.74	11.19	133.29	605.40
	2009	37.98	30.03	92.97	130.09	10.60	34.27	5.30	2.79	16.39	14.07	8.11	5.69	1.72	19.97	12.58	2.97	1.54	10.12	4.71	9.04	122.95	573.90
	2010	41.68	29.73	95.11	137.49	10.55	35.72	5.02	3.57	18.09	16.70	9.18	5.73	5.66	22.27	13.55	4.72	1.68	11.52	5.25	9.24	136.04	618.48
	2011	42.77	32.88	100.58	143.53	9.70	34.82	4.62	4.04	20.27	15.64	8.66	4.73	3.69	20.76	12.14	3.80	1.74	10.63	4.71	10.18	136.69	626.59
	2012	37.32	31.30	99.54	143.02	9.00	34.87	5.12	3.91	18.58	16.76	8.83	4.69	3.66	21.78	12.83	3.73	1.74	10.60	4.66	10.02	133.29	615.25
	2013	41.67	30.58	100.97	141.25	9.22	34.57	4.71	4.08	18.28	16.72	9.20	4.95	3.51	20.56	13.55	3.99	1.67	10.60	4.74	10.07	136.58	621.47
	2014	43.88	36.12	98.12	145.22	9.96	35.06	4.71	4.15	20.33	17.37	8.88	5.04	4.40	21.88	12.91	4.38	1.75	10.68	5.01	10.21	136.95	637.00
	2015	40.49	33.88	108.45	151.17	10.68	37.63	5.03	4.02	18.98	16.26	9.53	5.08	5.01	22.66	13.53	4.44	1.62	11.30	4.67	9.43	138.12	652.00
	2016	40.52	34.20	103.31	150.59	10.92	36.13	5.02	3.83	18.12	17.63	8.31	4.67	4.03	23.29	13.03	4.08	1.74	10.75	4.73	9.99	147.83	652.73
	2017	43.53	35.52	103.75	152.52	11.33	37.60	5.16	4.03	20.07	18.56	8.52	5.36	4.21	23.31	13.59	4.41	1.69	10.49	4.71	10.15	143.58	662.07
Unconnected lakes	2008	26.82	41.86	70.98	43.82	6.33	41.24	0.47	6.70	18.38	14.56	6.69	35.10	10.35	74.83	50.60	49.08	11.98	29.50	4.23	2.57	140.42	686.53
	2009	23.35	39.37	69.41	45.41	4.81	43.00	0.39	6.98	20.79	15.36	9.07	32.56	11.07	76.41	52.10	41.80	12.21	30.87	3.97	2.49	131.63	673.04
	2010	27.08	40.69	70.78	46.96	5.64	47.24	0.80	7.37	18.78	15.87	6.79	31.20	14.81	81.97	51.83	42.87	12.71	32.76	4.44	2.49	136.12	699.22
	2011	25.00	37.62	71.65	47.79	4.44	45.79	0.31	7.75	21.42	19.76	6.96	36.65	12.78	76.13	49.16	42.63	13.64	32.59	4.52	2.34	136.05	694.98
	2012	22.41	36.80	71.23	47.75	3.74	44.13	0.50	7.69	17.44	18.48	6.82	35.15	12.04	80.71	49.92	43.22	11.92	31.53	4.54	2.37	132.53	680.92
	2013	26.10	44.59	74.81	50.85	4.09	44.52	0.59	7.67	18.68	15.55	6.83	32.09	12.34	75.20	52.98	43.75	12.69	32.77	4.62	2.51	138.07	701.31
	2014	27.27	45.69	75.92	48.65	4.31	45.85	0.43	7.52	25.69	18.54	7.08	32.55	12.29	74.40	50.92	41.74	13.19	34.26	5.38	2.60	140.03	714.33
	2015	25.76	43.60	81.11	50.30	5.76	46.08	0.47	7.76	19.29	19.15	7.66	36.54	13.44	71.98	51.92	43.66	11.96	34.20	5.23	2.30	141.40	719.59
	2016	25.14	44.34	74.76	50.30	6.06	45.39	0.49	7.70	19.24	17.77	9.57	35.81	13.91	73.09	49.91	40.66	12.79	35.15	5.26	2.35	143.38	713.11
	2017	27.19	51.42	74.96	51.59	6.54	37.95	0.46	8.06	20.81	17.52	9.66	39.34	12.68	76.53	49.76	43.57	11.91	34.45	4.27	2.56	141.22	722.44

Table A3. ~~Area~~Areas of different sizes of glacial lakes in 2017 for some regions with large area growth of rates. The unit of area is km^2.

Lake grid ID (Mountain ranges)	69 (N)	116 (CH)	274 (WH)	71 (N)	48 (H)	74 (N)	72 (N)	14 (EH)	13 (EH)	39 (CH)	15 (EH)
≤0.01 km^2	0.18	0.28	0.20	0.16	0.22	0.16	0.17	0.23	0.16	0.32	0.33
0.01 km^2–0.02 km^2	0.85	1.51	1.29	0.71	1.43	1.08	1.37	1.45	1.45	1.49	2.46
0.02 km^2–0.04 km^2	1.69	2.16	2.22	1.79	3.24	2.09	2.29	2.24	2.06	2.72	4.14
0.04 km^2–0.08 km^2	1.78	3.19	2.98	2.20	5.30	3.38	4.45	2.77	2.69	3.66	7.16
0.08 km^2–0.16 km^2	1.91	5.38	3.87	2.86	4.81	4.03	5.06	3.75	4.33	5.00	13.16
0.16 km^2–0.32 km^2	1.81	4.53	2.23	2.76	4.62	5.55	5.81	2.91	3.90	5.66	11.62
0.32 km^2–0.64 km^2	1.01	5.37	1.77	1.79	3.88	1.75	3.81	5.72	3.99	7.13	12.37
0.64 km^2–1.28 km^2	0.00	2.94	0.00	1.38	2.82	2.96	4.43	0.96	7.10	8.97	7.74
≥1.28 km^2	0.00	7.22	4.19	0.00	11.46	3.17	2.59	6.07	1.40	6.06	12.00
Total area (km^2)	9.22	32.58	18.76	13.66	37.76	24.17	29.99	26.10	27.09	41.00	70.96
Total area (≤0.16 km^2)	6.41	12.52	10.57	7.72	14.99	10.74	13.35	10.45	10.69	13.18	27.24
% of Total area (≤0.16 km^2)	69.47	38.43	56.32	56.56	39.70	44.45	44.52	40.03	39.47	32.15	38.39
Annual area increase ($km^2\ a^{-1}$)	0.23	0.28	0.28	0.29	0.32	0.41	0.42	0.49	0.70	0.74	0.94

Table A4. Summary of correlation coefficients (*R*) for key lake topographic, geomorphic, and climatological parameters, calculated within 1° × 1° grid cells across HMA. Correlation coefficients are bold where $p < 0.05$; (*) indicates $p < 0.01$.

	Lake area (2008)	Lake area (2017)	Lake change (2008–2017)	Glacier (gl.) area ^	Debris-covered gl. area	Total gl. length	Mean gl. slope	Mean gl. elevation	Temperature change^^ 1979–2017	Precipitation change 1979–2017
Lake area (2008)	1.00									
Lake area (2017)	**0.99***	1.00								
Lake change (2008–2017)	**0.82***	**0.87***	1.00							
Glacier (gl.) area	**0.23***	**0.24***	**0.22***	1.00						
Debris-covered gl. area	**0.35***	**0.36***	**0.34***	**0.85***	1.00					
Total gl. length	**0.32***	**0.32***	**0.28***	**0.90***	**0.85***	1.00				
Mean gl. Slope	0.07	0.07	0.05	0.02	**0.18**	0.06	1.00			
Mean gl. Elevation	0.12	0.14	**0.17**	0.11	0.00	0.05	**−0.28***	1.00		
Temperature change 1979–2017	−0.09	−0.07	0.10	**−0.17**	**−0.25***	**−0.27***	0.00	0.07	1.00	
Precipitation change	−0.03	−0.01	0.09	−0.13	**−0.16**	**−0.15**	**−0.18***	**0.15**	**0.16**	1.00

^ Glacier data are derived from the Randolph Glacier Inventory (RGI Consortium, 2017), except for debris cover (after Scherler et al., 2018). Climate data are for ERA Interim.

^^ ERA-Interim near surface temperature and precipitation fields for the period 1979–2017 were obtained from the KNMI climate explorer (https://climexp.knmi.nl).

Table A5. Regional summary of key topographic, geomorphic, and climatological parameters compared to proglacial and supraglacial lake area in 2017. Correlation coefficients are bold where $p < 0.05$; (*) indicates $p < 0.01$.

Region	Total area (km^2)	Lake area (km^2)	Glacier (gl.) area (km^2)	Debris-covered gl. area (km^2)	Total gl. length (km)	Mean gl. slope (°)	Mean gl. elevation (m)	Temperature change 1979–2017 (°C/century)	Precipitation change 1979–2017
Central Himalaya	254886	155.7	8678	1567	10669	26	5542	2.77	−0.25
Central Tien Shan	105456	19.0	7270	842	7415	27	4181	1.35	0.05
Dzhungarsky Alatau	37542	10.3	521	18	978	24	3615	1.85	0.74
Eastern Himalaya	164785	104.7	2838	357	3614	24	5484	3.26	−0.84
Eastern Hindu Kush	95404	43.6	2938	609	5062	25	4856	0.08	−0.86
Eastern Kunlun Shan	256729	4.2	2995	45	3384	24	5389	3.60	0.06
Eastern Pamir	39605	5.2	2118	291	2364	27	5064	3.42	−0.50
Eastern Tibetan Mountains	333123	1.8	312	12	483	24	5345	3.55	0.73
Eastern Tien Shan	140900	8.7	2332	193	3977	28	3974	2.65	0.17
Gangdise Mountains	154884	23.2	1271	80	2570	24	5892	2.42	0.33
Hengduan Shan	372649	13.6	1281	212	2048	23	5278	2.24	−0.13
Karakoram	83644	11.7	21474	2013	16460	31	5399	2.37	−0.35
Northern/Western Tien Shan	187275	20.1	2262	223	4138	23	3943	3.22	−0.36

Nyainqêntanglha	172746	144.6	7047	1011	8710	25	5282	2.37	−1.00
Pamir Alay	71845	4.0	1847	319	3441	25	4109	3.88	−0.27
Qilian Shan	201699	4.7	1598	30	2588	26	4847	4.07	0.51
Tanggula Shan	145064	10.6	1841	84	1893	21	5521	3.34	0.46
Tibetan Interior Mountains	526111	4.4	3815	59	4179	23	5927	2.64	0.31
Western Himalaya	189494	36.3	7986	1149	11974	24	5180	1.93	−1.24
Western Kunlun Shan	123388	5.3	8457	159	8108	26	5642	3.22	−0.55
Western Pamir	109239	37.9	8417	1118	11640	27	4844	1.61	0.08
Lake area: Correlation Coefficient (*R*)			0.21	**0.50**	0.36	0.01	0.23	−0.17	**−0.49**
Excl. Karakoram			**0.49**	**0.72***	**0.52**	0.10	0.25	−0.18	**−0.50**

Table A6. Statistical results of stratified random sampling.

Stratum	Total pixel number	Total area (km^2)	No. of samples	No. of non-glacial lake samples	No. of glacial lake samples	No. of ambiguous samples
C0W0	2,022,448,650	1,820,203.78	1300	1215	37	48
C0W1	925,449	832.90	700	307	362	31
C1W0	814,196	732.77	700	21	678	1
C1W1	1,611,668	1450.50	1300	25	1260	15

Author contributions. FC: conceptualization, methodology, lake evolution analysis, project administration, resources, and writing; MMZ: conceptualization, methodology, lake evolution analysis, validation, and writing; HDG: funding acquisition, supervision, and writing; SA: methodology, climate and debris-cover analysis, validation, and writing; JSK: analysis, interpretation, and writing; UH: writing and interpretation; CSW: writing.

Competing interests. The authors declare that they have no conflict of interest.

Acknowledgments. We thank T. Bolch, and D. Shugar for their contributions to this project in its stages of development; L. Wang, S. G. Xu, Z. Y. Lin, H. Zhao, Y. H. Z. He, T. C. Shan, Z. W. Xu, N. Wang, Z. Z. Yin, and J. X. Wang for the cross-validations of the data that were so integral to this project.

Financial support. This work was supported by the Strategic Priority Research Program of the Chinese Academy of Sciences (XDA19030101), the International Partnership Program of the Chinese Academy of Sciences (131211KYSB20170046/131C11KYSB20160061), and the National Natural Science Foundation of China (41871345). SA was supported by the EVOGLAC project under the Swiss National Science Foundation (IZLCZ2_169979/1).

References

Aggarwal, S., Rai, S. C., Thakur, P. K., and Emmer, A.: Inventory and recently increasing GLOF susceptibility of glacial lakes in Sikkim, Eastern Himalaya, Geomorphology, 295, 39-54, https://doi.org/10.1016/j.geomorph.2017.06.014, 2017.

Armstrong, W. H., and Anderson, R. S.: Ice-marginal lake hydrology and the seasonal dynamical evolution of Kennicott Glacier, Alaska, Journal of Glaciology, 1-15, https://doi.org/10.1017/jog.2020.41, 2020.

Ashraf, A., Naz, R., and Roohi, R.: Glacial lake outburst flood hazards in Hindukush, Karakoram and Himalayan Ranges of Pakistan: implications and risk analysis, Geomatics, Natural Hazards and Risk, 3, 113-132, https://doi.org/10.1080/19475705.2011.615344, 2012.

Baumann, F., Jinsheng, H. E., Karsten, S., Peter, K., and Thomas, S.: Pedogenesis, permafrost, and soil moisture as controlling factors for soil nitrogen and carbon contents across the Tibetan Plateau, Global Change Biology, 15, 3001–3017, https://doi.org/10.1111/j.1365-2486.2009.01953.x, 2009.

Bhardwaj, A., Singh, M. K., Joshi, P. K., Snehmani, Singh, S., Sam, L., Gupta, R. D., and Kumar, R.: A lake detection algorithm (LDA) using Landsat 8 data: A comparative approach in glacial environment, International Journal of Applied Earth Observation & Geoinformation, 38, 150-163, https://doi.org/10.1016/j.jag.2015.01.004, 2015.

Bolch, T., Kulkarni, A., Kääb, A., Huggel, C., Paul, F., Cogley, J. G., Frey, H., Kargel, J. S., Fujita, K., and Scheel, M.: The state and fate of Himalayan glaciers, Science, 336, 310-314, https://doi.org/10.1126/science.1215828, 2012.

Brun, F., Berthier, E., Wagnon, P., Kääb, A., and Treichler, D.: A spatially resolved estimate of High Mountain Asia glacier mass balances from 2000 to 2016, Nature Geoscience, 10, 668-673, https://doi.org/10.1038/NGEO2999, 2017.

Capps, D. M., Wiles, G. C., Clague, J. J., and Luckman, B. H.: Tree-ring dating of the nineteenth-century advance of Brady Glacier and the evolution of two ice-marginal lakes, Alaska, The Holocene, 21, 641-649, https://doi.org/10.1177/0959683610391315, 2011.

Chen, F., Zhang, M., Tian, B., and Li, Z.: Extraction of glacial lake outlines in Tibet Plateau using Landsat 8 imagery and Google Earth Engine, IEEE Journal of Selected Topics in Applied Earth Observations & Remote Sensing, 10, 4002-4009, https://doi.org/10.1109/JSTARS.2017.2705718, 2017.

Chen, F., Zhang, M., Guo, H., Allen, S., Kargel, J., Haritashya, U., Watson, S.: Annual 30-meter Dataset for Glacial Lakes in High Mountain Asia from 2008 to 2017 (Hi-MAG) [Dataset], Zenodo, https://doi.org/10.5281/zenodo.4275164.

Chen, J., Zhu, X., Vogelmann, J. E., Gao, F., and Jin, S.: A simple and effective method for filling gaps in Landsat ETM+ SLC-off images, Remote Sensing of Environment, 115, 1053-1064, https://doi.org/10.1016/j.rse.2010.12.010, 2011.

Gardelle, J., Berthier, E., and Arnaud, Y.: Slight mass gain of Karakoram glaciers in the early twenty-first century, Nature Geoscience, 5, 322-325, https://doi.org/10.1038/ngeo1450, 2012.

Gardelle, J., Berthier, E., Arnaud, Y., and Kääb, A.: Region-wide glacier mass balances over the Pamir-Karakoram-Himalaya during 1999-2011, The Cryosphere, 7, 1263-1286, https://doi.org/10.5194/tc-7-1263-2013, 2013.

Gardner, A. S., Moholdt, G., Cogley, J. G., Wouters, B., Arendt, A. A., Wahr, J., Berthier, E., Hock, R., Pfeffer, W. T., and Kaser, G.: A reconciled estimate of glacier contributions to sea level rise: 2003 to 2009, Science, 340, 852, https://doi.org/10.1126/science.1234532, 2013.

Harrison, S., Kargel, J. S., Huggel, C., Reynolds, J., Dan, H. S., Betts, R. A., Emmer, A., Glasser, N., Haritashya, U. K., and Klimeš, J.: Climate change and the global pattern of moraine-dammed glacial lake outburst floods, Cryosphere, 12, 1-28, https://doi.org/10.5194/tc-12-1195-2018, 2018.

Immerzeel, W. W., and Bierkens, M. F. P.: Seasonal prediction of monsoon rainfall in three Asian river basins: the importance of snow cover on the Tibetan Plateau, International Journal of Climatology, 30, 1835–1842, https://doi.org/10.1002/joc.2033, 2010.

Kääb, A., Treichler, D., Nuth, C., and Berthier, E.: Brief communication: Contending estimates of 2003-2008 glacier mass balance over the Pamir-Karakoram-Himalaya, Cryosphere, 9, 557-564, https://doi.org/10.5194/tc-9-557-2015, 2015.

King, O., Bhattacharya, A., Bhambri, R., and Bolch, T.: Glacial lakes exacerbate Himalayan glacier mass loss, Scientific Reports, 9, 18145, https://doi.org/10.1038/s41598-019-53733-x, 2019.

Krumwiede, B. S., Kamp, U., Leonard, G. J., Kargel, J. S., Dashtseren, A., and Walther, M.: Recent glacier changes in the Mongolian Altai Mountains: Case studies from Munkh Khairkhan and Tavan Bogd, Global Land Ice Measurements from Space, https://doi.org/10.1007/978-3-540-79818-7_22, 2014.

Li, D., Shangguan, D., and Naveed, A. M.: Glacial lake inventory derived from Landsat 8 OLI in 2016–2018 in China–Pakistan economic corridor, International Journal of Geo-Information, 9, 294, https://doi.org/10.3390/ijgi9050294, 2020.

Li, J., and Sheng, Y.: An automated scheme for glacial lake dynamics mapping using Landsat imagery and digital elevation models: A case study in the Himalayas, International Journal of Remote Sensing, 33, 5194-5213, https://doi.org/10.1080/01431161.2012.657370, 2012.

Liu, J. J., Cheng, Z. L., and Su, P. C.: The relationship between air temperature fluctuation and Glacial Lake Outburst Floods in Tibet, China, Quaternary International, 321, 78-87, https://doi.org/10.1016/j.quaint.2013.11.023, 2014.

Luo, W., Zhang, G., Chen, W., and Xu, F.: Response of glacial lakes to glacier and climate changes in the western Nyainqentanglha range, Science of The Total Environment, 735, 139607, https://doi.org/10.1016/j.scitotenv.2020.139607, 2020.

Miles, E. S., Steiner, J., Willis, I., Buri, P., Immerzeel, W. W., Chesnokova, A., and Pellicciotti, F.: Pond dynamics and supraglacial-englacial connectivity on debris-covered Lirung Glacier, Nepal, Frontiers in Earth Science, 5, https://doi.org/10.3389/feart.2017.00069, 2017a.

Miles, E. S., Willis, I. C., Arnold, N. S., Steiner, J., and Pellicciotti, F.: Spatial, seasonal and interannual variability of supraglacial ponds in the Langtang Valley of Nepal, 1999–2013, Journal of Glaciology, 63, 88-105, https://doi.org/10.1017/jog.2016.120, 2017b.

Mueller, N., Lewis, A., Roberts, D., Ring, S., Melrose, R., Sixsmith, J., Lymburner, L., Mcintyre, A., Tan, P., and Curnow, S.: Water observations from space: Mapping surface water from 25 years of Landsat imagery across Australia, Remote Sensing of Environment, 174, 341-352, https://doi.org/10.1016/j.rse.2015.11.003, 2016.

Neckel, N., Kropáček, J., Bolch, T., and Hochschild, V.: Glacier mass changes on the Tibetan Plateau 2003-2009 derived from ICESat laser altimetry measurements, Environmental Research Letters, 9, 468-475, https://doi.org/10.1088/1748-9326/9/1/014009, 2014.

Nie, Y., Sheng, Y., Liu, Q., Liu, L., Liu, S., Zhang, Y., and Song, C.: A regional-scale assessment of Himalayan glacial lake changes using satellite observations from 1990 to 2015, Remote Sensing of Environment, 189, 1-13, https://doi.org/10.1016/j.rse.2016.11.008, 2017.

Pekel, J. F., Cottam, A., Gorelick, N., and Belward, A. S.: High-resolution mapping of global surface water and its long-term changes, Nature, 540, 418-422, https://doi.org/10.1038/nature20584, 2016.

Qiao, L., Guo, W., Yong, N., Liu, S., and Xu, J.: Recent glacier and glacial lake changes and their interactions in the Bugyai Kangri, southeast Tibet, Annals of Glaciology, 57, 61-69, https://doi.org/10.3189/2016AoG71A415, 2016.

Quincey, D. J., Richardson, S. D., Luckman, A., Lucas, R. M., Reynolds, J. M., Hambrey, M. J., and Glasser, N. F.: Early recognition of glacial lake hazards in the Himalaya using remote sensing datasets, Global & Planetary Change, 56, 137-152, https://doi.org/10.1016/j.gloplacha.2006.07.013, 2007.

RGI-Consortium: Randolph Glacier Inventory - a dataset of global glacier outlines: Version 6.0: Technical report, Global Land Ice Measurements from Space, https://doi.org/10.7265/N5-RGI-60, 2017.

Richardson, S. D., and Reynolds, J. M.: An overview of glacial hazards in the Himalayas, Quaternary International, 65-66, 31-47, https://doi.org/10.1016/S1040-6182(99)00035-X, 2000.

Rounce, D., Watson, C. S., and Mckinney, D.: Identification of hazard and risk for glacial lakes in the Nepal Himalaya using satellite imagery from 2000–2015, Remote Sensing, 9, 654, https://doi.org/10.3390/rs9070654, 2017.

Salerno, F., Thakuri, S., D'Agata, C., Smiraglia, C., Manfredi, E. C., Viviano, G., and Tartari, G.: Glacial lake distribution in the Mount Everest region: Uncertainty of measurement and conditions of formation, Global & Planetary Change, 92-93, 30-39, https://doi.org/10.1016/j.gloplacha.2012.04.001, 2012.

Scherler, D., Bookhagen, B., and Strecker, M. R.: Spatially variable response of Himalayan glaciers to climate change affected by debris cover, Nature Geoscience, 4, 156-159, https://doi.org/10.1038/ngeo1068, 2011.

Scherler, D., Wulf, H., and Gorelick, N.: Global assessment of supraglacial debris-cover extents, Geophysical Research Letters, 45, 11798-11805, https://doi.org/10.1029/2018GL080158, 2018.

Schiemann, R., Lüthi, D., and Schär, C.: Seasonality and interannual variability of the westerly jet in the Tibetan Plateau region, Journal of Climate, 22, 2940-2957, https://doi.org/10.1175/2008JCLI2625.1, 2009.

Sen, P. K.: Estimates of the regression coefficient based on Kendall's Tau, Journal of the American Statistical Association, 63, 1379-1389, https://doi.org/10.1080/01621459.1968.10480934, 1968.

Shugar, D. H., and Clague, J. J.: The sedimentology and geomorphology of rock avalanche deposits on glaciers, Sedimentology, 58, 1762-1783, https://doi.org/10.1111/j.1365-3091.2011.01238.x, 2011.

Shugar, D. H., Burr, A., Haritashya, U. K., Kargel, J. S., Watson, C. S., Kennedy, M. C., Bevington, A. R., Betts, R. A., Harrison, S., and Strattman, K.: Rapid worldwide growth of glacial lakes since 1990, Nature Climate Change, 10, 939-945, https://doi.org/10.1038/s41558-020-0855-4, 2020.

Song, C., Sheng, Y., Ke, L., Nie, Y., and Wang, J.: Glacial lake evolution in the southeastern Tibetan Plateau and the cause of rapid expansion of proglacial lakes linked to glacial-hydrogeomorphic processes, Journal of Hydrology, 540, 504-514, https://doi.org/10.1016/j.jhydrol.2016.06.054, 2016.

Song, C., Sheng, Y., Wang, J., Ke, L., Madson, A., and Nie, Y.: Heterogeneous glacial lake changes and links of lake expansions to the rapid thinning of adjacent glacier termini in the Himalayas, Geomorphology, 280, 30-38, https://doi.org/10.1016/j.geomorph.2016.12.002, 2017a.

Song, X. P., Potapov, P. V., Krylov, A., King, L. A., Bella, C. M. D., Hudson, A., Khan, A., Adusei, B., Stehman, S. V., and Hansen, M. C.: National-scale soybean mapping and area estimation in the United States using medium resolution satellite imagery and field survey, Remote Sensing of Environment, 190, 383-395, https://doi.org/10.1016/j.rse.2017.01.008, 2017b.

Song, X. P., Hansen, M. C., Stehman, S. V., Potapov, P. V., Tyukavina, A., Vermote, E. F., and Townshend, J. R.: Global land change from 1982 to 2016, Nature, 560, 639-643, https://doi.org/10.1038/s41586-018-0411-9, 2018.

Stehman, S. V.: Impact of sample size allocation when using stratified random sampling to estimate accuracy and area of land-cover change, Remote Sensing Letters, 3, 111-120, https://doi.org/10.1080/01431161.2010.541950, 2012.

Sudan, B. M., Pradeep, K. M., Wu, L., Gao, X., Finu, S., Rajendra, B. S., Narendra, R. K., Samjwal, R. B., Sharad, J., Sonika, S., and Prasant, B.: The status of glacial lakes in the Hindu Kush Himalaya-ICIMOD Research Report 2018/1, 2018.

Thakuri, S., Salerno, F., Bolch, T., Guyennon, N., and Tartari, G.: Factors controlling the accelerated expansion of Imja Lake, Mount Everest region, Nepal, Annals of Glaciology, 57, 245-257, https://doi.org/10.3189/2016AoG71A063, 2016.

Thompson, S. S., Benn, D. I., Dennis, K., and Luckman, A.: A rapidly growing moraine-dammed glacial lake on Ngozumpa Glacier, Nepal, Geomorphology, 145, 1-11, https://doi.org/10.1016/j.geomorph.2011.08.015, 2012.

Truffer, M., and Motyka, R. J.: Where glaciers meet water: Subaqueous melt and its relevance to glaciers in various settings, Reviews of Geophysics, 54, 220-239, https://doi.org/10.1002/2015RG000494, 2016.

Ukita, J., Narama, C., Tadono, T., Yamanokuchi, T., Tomiyama, N., Kawamoto, S., Abe, C., Uda, T., Yabuki, H., and Fujita, K.: Glacial lake inventory of Bhutan using ALOS data: methods and preliminary results, Annals of Glaciology, 52, 65-71, https://doi.org/10.3189/172756411797252293, 2011.

Umesh, H., Jeffrey, K., Dan, S., Gregory, L., Katherine, S., Watson, C., David, S., Stephan, H., Kyle, M., and Dhananjay, R.: Evolution and controls of large glacial lakes in the Nepal Himalaya, Remote Sensing, 10, 798-, https://doi.org/10.3390/rs10050798, 2018.

Wang, N., Chen, F., Yu, B., and Qin, Y.: Segmentation of large-scale remotely sensed images on a Spark platform: A strategy for handling massive image tiles with the MapReduce model, ISPRS Journal of Photogrammetry and Remote Sensing, 162, 137-147, https://doi.org/10.1016/j.isprsjprs.2020.02.012, 2020a.

Wang, X., Ding, Y., Liu, S., Jiang, L., Wu, K., Jiang, Z., and Guo, W.: Changes of glacial lakes and implications in Tian Shan, central Asia, based on remote sensing data from 1990 to 2010, Environmental Research Letters, 8, 575-591, https://doi.org/10.1088/1748-9326/8/4/044052, 2013.

Wang, X., Guo, X., Yang, C., Liu, Q., Wei, J., Zhang, Y., Liu, S., Zhang, Y., Jiang, Z., and Tang, Z.: Glacial lake inventory of High Mountain Asia (1990-2018) derived from Landsat images, Earth System Science Data, 1-23, https://doi.org/10.5194/essd-2019-212, 2020b.

Xu, H.: Modification of normalised difference water index (NDWI) to enhance open water features in remotely sensed imagery, International Journal of Remote Sensing, 27, 3025-3033, https://doi.org/10.1080/01431160600589179, 2006.

Yao, T., Thompson, L., Yang, W., Yu, W., Yang, G., Guo, X., Yang, X., Duan, K., Zhao, H., and Xu, B.: Different glacier status with atmospheric circulations in Tibetan Plateau and surroundings, Nature Climate Change, 2, 663-667, https://doi.org/10.1038/nclimate1580, 2012.

Yu, B., Chen, F., and Xu, C.: Landslide detection based on contour-based deep learning framework in case of national scale of Nepal in 2015, Computers & Geosciences, 135, 104388, https://doi.org/10.1016/j.cageo.2019.104388, 2020.

Zhang, G., Yao, T., Xie, H., Wang, W., and Yang, W.: An inventory of glacial lakes in the Third Pole region and their changes in response to global warming, Global & Planetary Change, 131, 148-157, https://doi.org/10.1016/j.gloplacha.2015.05.013, 2015.

Zhang, M., Chen, F., Tian, B., Liang, D., and Yang, A.: High-frequency glacial lake mapping using time series of sentinel-1A/1B SAR imagery: An assessment for the southeastern Tibetan Plateau, International Journal of Environmental Research and Public Health, 17, 1072, https://doi.org/10.3390/ijerph17031072, 2020.

Zhao, B., Wang, Y., Luo, Y., Liang, R., Li, J., and Xie, L.: Large landslides at the northeastern margin of the Bayan Har Block, Tibetan Plateau, China, Royal Society Open Science, 6, 180844, https://doi.org/10.1098/rsos.180844, 2019.

Zhao, H., Chen, F., and Zhang, M.: A systematic extraction approach for mapping glacial lakes in High Mountain regions of Asia, IEEE Journal of Selected Topics in Applied Earth Observations and Remote Sensing, 11, 2788-2799, https://doi.org/10.1109/JSTARS.2018.2846551, 2018.

Zhu, Z., and Woodcock, C. E.: Object-based cloud and cloud shadow detection in Landsat imagery, Remote Sensing of Environment, 118, 83-94, https://doi.org/10.1016/j.rse.2011.10.028, 2012.